Map and Description of the Active Part of the Slumgullion Landslide, Hinsdale County, Colorado

By
Robert W. Fleming *and* Rex L. Baum, U.S. Geological Survey, *and*
Marco Giardino, Consiglio Nazionale Delle Ricerche—Centro Studi

1999

U.S. DEPARTMENT OF THE INTERIOR

U.S. GEOLOGICAL SURVEY

CONTENTS

FIGURES

Map and Description of the Active Part of the Slumgullion Landslide, Hinsdale County, Colorado

By

Robert W. Fleming *and* Rex L. Baum, U.S. Geological Survey, *and*

Marco Giardino, Consiglio Nazionale Delle Ricerche—Centro Studi

ABSTRACT

This text accompanies a map of many of the features on the active part of the Slumgullion landslide, Hinsdale County, Colo. Long-term movement creates and destroys a variety of structural features on the surface of the landslide including faults, fractures, and folds, as well as basins and ridges.

The Slumgullion landslide consists of a large volume of inactive landslide deposits and a much smaller volume that is actively moving within the deposits of the older landslide. Previously, collapse of the south side of the scarp on Mesa Seco produced materials that blocked the Lake Fork of the Gunnison River and created Lake San Cristobal. The current landslide activity was triggered by a collapse, which apparently extended the pre-existing headscarp toward the north. The loading induced by the deposition of the collapsed materials reactivated some of the older landslide deposits.

Displacement rates in the active part of the landslide range from about 0.2 m/yr at the uppermost fractures to a maximum of 7.4 m/yr in the narrowest part of the landslide. From this maximum rate, displacement rate declines to 2 or less m/yr at the toe. The interplay between different displacement rates, varying width, and curving boundaries gives rise to the structures within the landslide.

For purposes of description, the landslide has been divided into seven zones: head, zone of stretching, the hopper and neck, zone of pull-apart basins, pond deposits and emergent toe, zone of shortening and spreading, and active toe. Each zone has its characteristic kinematic expression that provides information on the internal deformation of the landslide. In general, the upper part of the landslide is characterized by features such as normal faults and tension cracks associated with stretching. The lowermost part of the landslide is characterized by thrust faults and other features associated with shortening. In between, features are a result of widening, bending, or narrowing of the landslide. Also, in places where the slope of the landslide is locally steeper than average, small landslides form on the surface of the larger landslide.

On the basis of qualitative observations of changes in the morphology and displacement, we speculate that the landslide is unlikely to accelerate and is more likely to stop movement over a time scale of decades. This speculation is based on the observation that driving forces are gradually diminishing and resisting forces are increasing. Rejuvenation or reactivation probably requires collapse of a new block in the head of the landslide.

INTRODUCTION

BACKGROUND AND PURPOSE

The Slumgullion landslide is in southwestern Colorado about 5 km southeast of the town of Lake City, Hinsdale County (figs. 1 and 2). The landslide is within the San Juan Mountains, and nearly all of the bedrock is of volcanic origin. Materials in the landslide deposit have been derived from the volcanic rocks. The Slumgullion landslide has a complex history of movement and currently consists of a large area of inactive landslide deposits and a smaller area that is active (fig. 2*A* and *B*). The currently active part of the landslide is itself complex; it consists of a variety of different materials moving at different rates along irregular boundaries. One of the more interesting aspects of the currently active landslide is that it has been moving for more than 100 yr, and observations during the 100 yr indicate that annual rates of movement might have been about constant throughout that time.
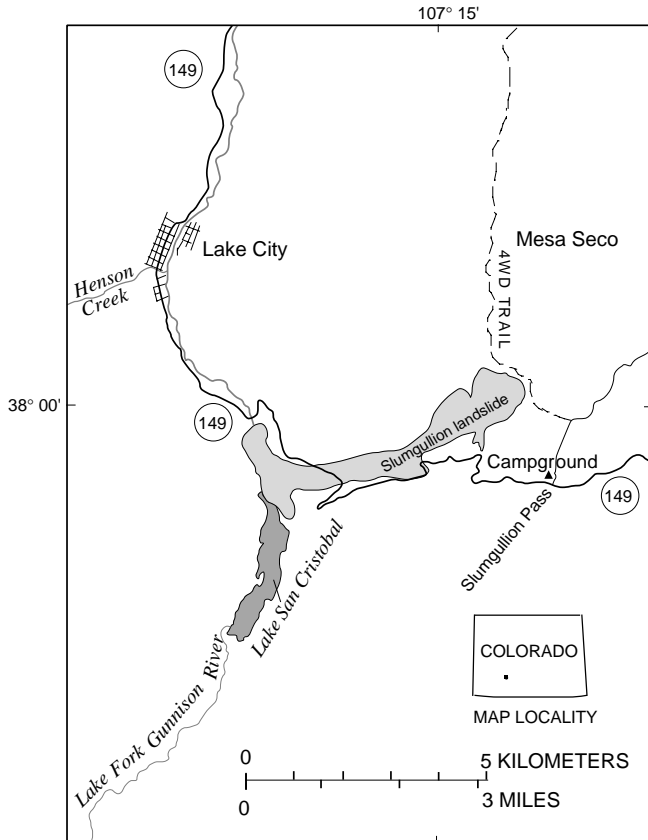
Figure 1. Index map showing location of the Slumgullion landslide. Shaded area outlines both the active and inactive parts of landslide.

The Slumgullion landslide has been described by several investigators, beginning with a short note by Endlich (1876) in the report of the Hayden Survey of 1874. The name "Slumgullion," already ascribed to the landslide by miners at the time of Endlich's (1876) description, is an old term referring to a meat stew containing many different ingredients and having a variegated appearance. The first published photograph of the landslide was by Whitman Cross (pl. XXB *in* Howe, 1909) and later mentioned in Atwood and Mather (1932) and Burbank (1947). The first investigation of the rates and history of movement was by Crandell and Varnes (1960, 1961). Rates of movement were monitored by resurveys of lines of stakes across the active landslide at several locations. Radiocarbon ages determined on wood fragments exposed at the toe of the inactive landslide provided an estimate of about 700 yr for the overall age of movement. Their estimate of age of the active part of the landslide, based on analysis of tree rings, was suggested to be about 300 yr.

The Colorado Geological Survey obtained aerial photographs of the Slumgullion landslide in 1985. In 1990, the U.S. Geological Survey began a comprehensive study of the Slumgullion landslide and obtained a new set of aerial photographs. The 1985 and 1990 aerial photographs were used by Smith (1993) to obtain displacement rates of different parts of the landslide from change in position of photo-identifiable points.

The study of the Slumgullion landslide by the U.S. Geological Survey includes geophysical investigations, precise surveying and leveling, history of movement, displacement rates, landslide kinematics, material properties, and landslide dams. Preliminary results of some of these investigations are in Varnes and Savage (1996). This map builds on information collected during the early part of the project by two exchange students from Italy (Parise and Guzzi, 1992; and Guzzi and Parise, 1992). They made estimates of the volume of the active and inactive parts of the landslide and demonstrated that detailed mapping of the active part of the landslide could provide useful information about the kinematics of movement. Some of the descriptions presented herein were published as part of a guidebook article for a field trip of the Geological Society of America at the 1996 Annual Meeting in Denver, Colo. (Fleming and others, 1996). The map has not been previously published.

Total elevation difference from the toe of the inactive part at the Lake Fork to the top of the 200-m-high scarp is about 1,000 m (3,400 ft), and the average slope of the surface is about 1:6, or 9°-10°. Excluding the height of the scarp, the average slope is about 7.5°. The length from top of scarp to the inactive toe at the level of Lake Fork is about 6 km (3.6 mi). Part of the inactive toe is under the water of Lake San Cristobal. When the landslide reached the valley floor of the Lake Fork, the toe spread both upstream and downstream. Maximum depth of Lake San Cristobal at the upstream terminus of the toe is 29.5 m (Crandell and Varnes, 1961). The deposit covers an area of 4.64 km² and has a volume estimated to be 170 million m³ (Parise and Guzzi, 1992).

The active part of the Slumgullion landslide is nearly completely surrounded by deposits of the inactive landslide (fig. 2). It covers an area of 1.46 km² and has a volume conservatively estimated at 20 million m³ (Parise and Guzzi, 1992).

The active part of the Slumgullion landslide is shown here on three map sheets that can be joined along match lines. This map is principally of

2
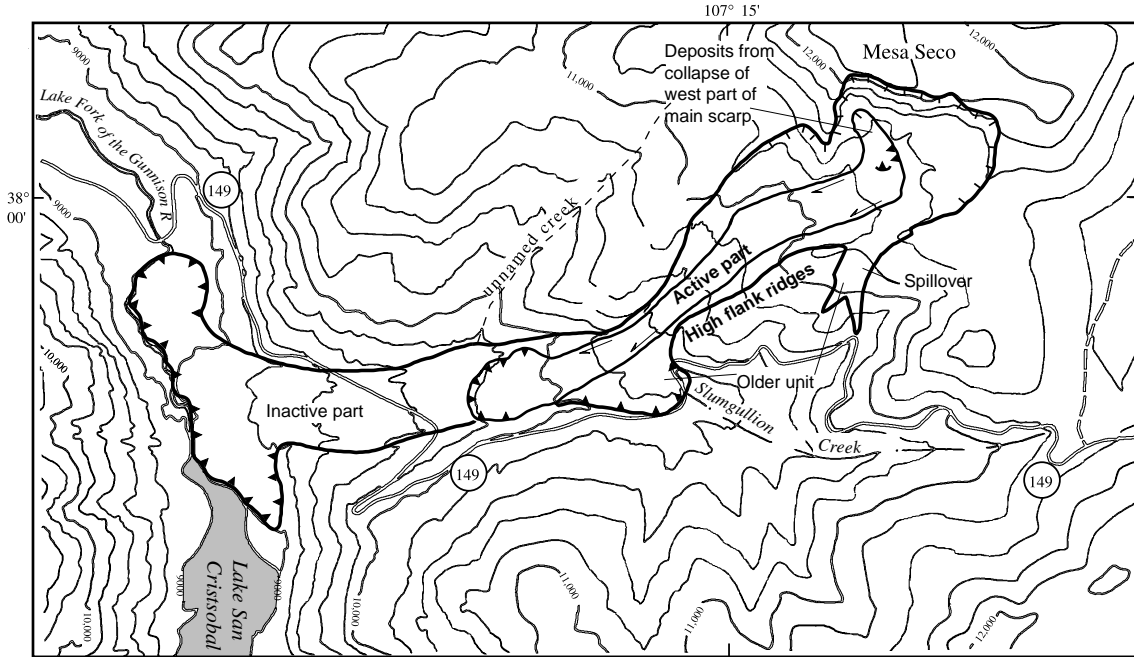
EXPLANATION

⊥⊥⊥ **Scarp**—Hachures point downhill

▲▲▲ **Toe**—Sawteeth on moving ground

⇌ **Flank**—Arrows show relative movement

0   **1** **KILOMETER**

0   **1 MILE**

contour interval = 200 ft
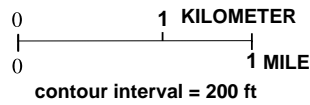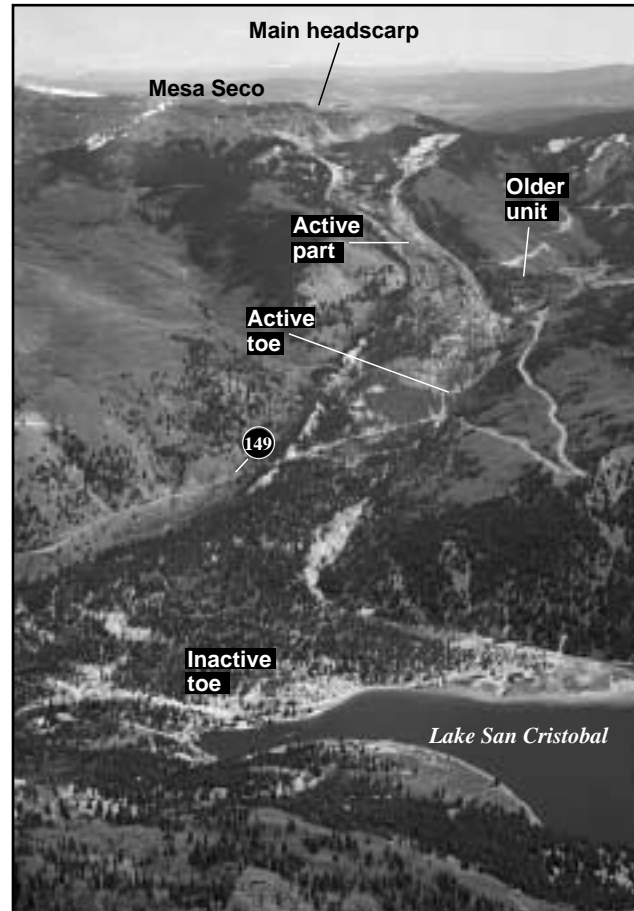
Figure 2. *A,* Outline map of inactive and active parts of the Slumgullion landslide. Inactive part of landslide is made up of materials that blocked Slumgullion Creek and spilled over a local topographic divide farther upslope, subsequently blocking the Lake Fork of Gunnison River and creating Lake San Cristobal. A collapse of west side of main scarp that provided a surcharge load to upper part of older landslide deposits apparently triggered currently active part of landslide. *B,* Aerial view of Slumgullion landslide, looking northeast (photograph by David Varnes).

3

structural features within the irregular boundaries of the active landslide. We have attempted to draw features such as faults and scarps and to report evidence of internal deformation such as split trees in order to depict the kinematics of movement and to understand the behavior of different parts of the landslide. The map also shows annual displacement at more than 300 places within and along the boundaries of the active landslide. We use the combined kinematic and displacement information to speculate on the future behavior of the landslide.

Fundamental tenets of this study of landslide structures are that the ground-surface expression of fractures and other deformational features are products of (1) local variations in boundary geometry, including the shape of the failure surface and of (2) position relative to driving and resisting elements within the landslide. Variations in boundary geometry produce a variety of structures such as pull-apart basins, grabens, and steps in faults that accommodate widening or narrowing of the landslide. These structures may have counterparts in much larger geologic structures in tectonic situations (Johnson and others, 1997). The idea of driving and resisting elements within a landslide comes from the limit-equilibrium method of stability analysis. The analysis evaluates driving and resisting forces within the landslide and compares resistance against sliding to forces promoting sliding. We believe that we can recognize these elements in the field on the basis of deformational behavior (in other words, stretching or shortening) of the landslide.

These tenets are important to landslide studies. The boundary geometry, including the position and shape of the failure surface, is an essential quantity together with strength parameters of the material and water-seepage conditions in the analysis of stability. Recognition of driving and resisting elements within the landslide may have application in improvements in methods of stability analysis (Baum and Fleming, 1991). If the properties and geometry are correctly expressed in a limit-equilibrium analysis, the positions of driving and resisting elements will also be correct. Thus, surface mapping and measurement of deformation have application to stability analysis as well as process studies.

TOPOGRAPHIC BASE

Base maps at a scale large enough to produce a map of landslide features at their true scale and position are generally unavailable and must be spe-cially made. For other large-scale specialized maps, we typically have prepared our base map by plane table or total-station survey techniques. (See, for example, Fleming and Johnson, 1989; Johnson and others, 1994; and Baum and others, 1993). For this project, the area was too large to prepare a detailed base map by traditional survey techniques. Rather, the base map was drawn from aerial photographs using an analytical stereoplotter that stored contour information digitally. Because this method is somewhat unusual in landslide studies, we describe the various steps involved.

An array of control points outside the boundaries of active movement was precisely surveyed by a field party under the leadership of David Varnes. Plastic panels in the form of crosses were centered on the control points, and in 1990 aerial photographs were obtained of the landslide area at scales of 1:14,000 and 1:6,000. The base map was prepared by James Messerich in the U.S. Geological Survey Plotter Lab from the 1:6,000-scale aerial photographs using a Kern DSR-1[1] analytical stereoplotter. Data were digitally stored with reference to the local coordinate system established by the Varnes survey. Base maps can be plotted at any scale from the digital data set; the 1:1,000 scale we adopted for mapping of landslide features was adequate given the density of fractures and quality of detail preserved in most places.

The landslide moved differentially, but as much as about 18 m, between the time the topography was mapped and the landslide features were mapped. The base map was made from aerial photographs taken during 1990, and our field mapping was completed during three 2-week intervals during 1992 and 1993. Positions of features to be mapped were based on the detailed form of the contour lines on the base map, and the topographic forms on moving ground were offset a variable amount with respect to nonmoving ground outside the landslide boundary. Even though the contour lines were displaced by slide movement, the form of contour lines was not visibly changed by movement between 1990 and 1993. Features generally could be located within a few meters on the ground. However, accurate locations were impossible in areas lacking distinctive topographic features and in areas of dense vegetation.

---

[1] Any use of trade, product, or firm names is for descriptive purposes only and does not imply endorsement by the U.S. Government.

WHAT IS SHOWN ON THE MAP

Most of the mapped features are indicators of deformation in the landslide. We separate **direct** and **indirect indicators** of deformation. Features such as faults and fractures are **direct indicators**. **Thrust faults**, whether within the boundaries of the landslide or along part of the landslide perimeter, are drawn with sawteeth on the overriding plate. Thrust faults are discontinuities that indicate shortening deformation, and in the nomenclature of landslides are called **landslide toes**. A thrust fault within the body of the landslide is termed an **internal toe** and is distinguished from the structure at the distal end of the landslide, the **toe**. A **fault scarp** is a purely descriptive structure that can represent normal faulting, strike-slip faulting, or oblique-slip faulting. In most cases it was impossible to ascertain the sense of slip along a scarp because of the crumbly nature of the landslide soils. The presence of the scarps combined with information from nearby displacement vectors and (or) indirect indicators of movement such as stretched roots or split trees can give a qualitative idea of sense of offset. Faults and scarps within the boundaries of the landslide are termed **internal faults** or **scarps. Tension cracks** are irregular, open gashes in the landslide surface. The surfaces of tension cracks are rough and irregular, indicating that they formed by pure opening. Also mapped are **en echelon cracks** that are small tension cracks whose pattern indicates shear deformation; left-stepping cracks indicate right-lateral shear and vice versa. And, finally, we use **fracture** as a general term to describe a break in the surface that is not identifiable as a tension crack or a fault. The sense of movement on a fracture is undefined unless indicated by an arrow. We believe that most fractures are strike-slip faults along the landslide boundary and oblique-slip faults within landslide boundaries. However, the crumbly nature of the soils at the surface of the landslide contributes to ambiguity in the interpretation of rupture type.

For all the mapped features, a solid line indicates that the feature is believed to be active and is accurately located. A dashed line indicates that the feature is apparently inactive, but the location is accurate. A dotted line indicates that the location and type of movement are inferred. In all cases, the locations were drawn with respect to the local topography on the landslide. The criteria used to distinguish between active and inactive features were imprecise. The presence of tiny cracks and evidence of active soil or plant disturbance made simple the recognition of active features. Where there was some question about activity, the presence of loose and crumbly soil at the ground surface was used as an indicator of active deformation. The soil surface on inactive features was typically a little stiff or crusty. There is minor cementation at the surface of inactive features that results from evaporation of water containing large amounts of dissolved solids. Active deformation tends to destroy this crust. Surfaces that have been undisturbed for relatively long periods of time contain a scattered covering of selenite crystals.

We also mapped several **indirect indicators** of deformation. **Highly fractured areas**, indicated by a hachured pattern, were outlined where individual fractures are too closely spaced to depict separately or where deformation is so intense that the surficial soils are dilated and soft. These highly fractured areas typically were found at intersections of fracture zones and at bends and curves in fracture zones. Areas mapped as **extrusion areas** are places where clay-rich material from the substrate, typically gray, white, yellow, or purple silty clay or clayey silt, has been extruded to the ground surface. The extrusion areas occur in several different kinematic situations within the active landslide. Boundaries of both the extrusion areas and highly fractured areas are indistinct, and thus the map units are subjective.

Other indirect indicators provide specific information about the kinematics of deformation. Shown on the map are the locations and orientations of **stretched tree roots**, **split trees**, and **small buckle folds**. These features are created by local deformation within boundaries of active movement and qualitatively depict the direction of maximum, one-dimensional strain on the landslide surface.

The fractures in the surface of the landslide are so informative that it is unfortunate more of the surface was not conducive to their formation and preservation. In places, particularly in the upper part of the landslide, there are large areas of cobble-to-boulder-size fragments of columnar-jointed rock. These areas do not show or preserve fractures of any type. Much of the remainder of the landslide is covered by a yellow, red, or brown clay-rich silt or silty clay that is soft and powdery when dry. Different kinds of fractures are preserved to different degrees in these materials. Movement that results in a scarp is generally identifiable; pure strike-slip movement is poorly expressed except on the landslide flanks where differential displacements are very large and materials are more moist. The small structures that we have used to understand the kinematics of other large landslides

(Fleming and Johnson, 1989) were preserved only in a few localized places where they formed in pond sediments or alluvium. In part, the presence of split trees and stretched tree roots have served as indicators of local deformation that could be obtained from the fractures in a more competent material.

Bearing in mind that the currently active part of the landslide may have been moving for about 300 yr, features such as scarps, pull-apart basins and thrust faults are created, transported, and destroyed by the movement. A mapped feature may have been caused by a condition that no longer exists where the feature exists. Or a similar feature may be being created at another place on the landslide. We know that some structures, such as listric faults and thrust faults, formed at specific parts of a pull-apart basin within the landslide. Continued movement transported these features downslope to positions where they are no longer active but are still recognizable. This aspect of the mapping, while a limitation where we did not recognize or understand a particular structure, allows improved interpretation of landslide behavior where we do recognize the structure. In the case of the pull-apart basin just mentioned, the recognition of the displaced features of the basin is evidence that the position of the basin is fixed, and structures are created in the basin and transported as inactive features downslope. We were able to recognize transported and inactive features more than 100 m downslope from the places where they had formed.

The map provides some information about locations of springs (where water seeps or flows onto the ground surface from the subsurface) and sinks (where water disappears into the soil or into cracks at the ground surface). Because the locations of springs and sinks were not a principal focus of this study, their depiction on the map is incomplete. Most springs having a discharge larger than a few liters/minute are shown.

We also show average annual **landslide displacement** on the map. Displacement vectors, shown as a red overprint on the map, were obtained by Smith (1993). The displacements were calculated from replicate measurements of positions of more than 300 identifiable points on aerial photographs that were taken in 1985 and 1990. Positions are known with an accuracy of about 1 m for the entire 5-yr interval between photographs. Thus, average annual rates, except for a few places of obvious errors in measurement, should typically be within about 20 cm/yr.

Displacement was also measured around the perimeter of the active landslide with wooden stakes and a tape measure. The locations of these measurement points and annual displacement are also shown on the map. Small dots indicate the approximate positions of the wooden stakes. The measurement of displacement around the perimeter was during the interval September 1992 to September 1993. The data obtained by the photogrammetric and direct methods were thus from different times, and the agreement in values seems remarkable.

At about the narrowest part of the landslide (shown on sheet 2), there is a line of six rebar rods that were installed by David Varnes as part of earlier displacement measurements. We surveyed the positions of the rods four times beginning in 1991 and last in 1996. The first survey was with a plane table and later surveys were with a total station. Not all the points were visible from the instrument station at the time of each survey, so there are a few gaps in the data set. We also located a 2 by 2-inch wooden stake near the left flank of the active landslide that had been installed more than 30 yr earlier (Crandell and Varnes, 1961); we located the end of that stake line and were able to obtain a 30-yr rate estimate (sheet 2).

There are a few other notes on the maps that identify locations of displacement and (or) deformation measurements. Positions of striped posts that were placed by the Bureau of Public Roads are shown on sheet 3. Locations of recording extensometers that are described in Savage and Fleming (1996) and locations of quadrilaterals that were placed in different parts of the landslide to determine local deformation are also shown.

HISTORY OF MOVEMENT

At least three separate events are recognizable in deposits of the Slumgullion landslide. Crandell and Varnes (1960, 1961) recognized an older, inactive deposit and a younger, active landslide (fig. 2). Our mapping has determined that the currently active landslide is a result of loading caused by collapse of the north side of the scarp on Mesa Seco. Thus, there are three clearly identifiable events, although the collapse of the north side of the scarp and reactivation of part of the old landslide was probably a continuous process.

Chleborad (1993) and Madole (1996) have studied different parts of the inactive landslide deposit and suggested there may be additional episodes of

movement. They used radiocarbon dating, differences in degree of weathering and soil formation, and morphology to separate ages of deposits. The two oldest deposits (fig. 2) occur (1) outside of the basin containing the Slumgullion landslide as a spillover that crossed a topographic divide at elevation 11,200 ft (3,677 m) and (2) as a lobe of deposit that blocked Slumgullion Creek at elevation 10,200 ft (3,349 m). The spillover site (Chleborad, 1993) contained wood that provides an estimated age of emplacement of about 1,000 to 1,300 yr before the present. Madole (1996) recognized well-developed soils formed on the lobe of the landslide that blocked Slumgullion Creek and along the outermost flank ridge on the south side of the inactive landslide. Both of these deposits appear to be from the earliest episode of movement. The oldest deposits are principally yellow to reddish-brown clay and seem to best match the exposed clays in the south side of the scarp area between 11,800 and 12,000 ft (3,874 and 3,940 m). Furthermore, the oldest deposits lack large concentrations of unaltered volcanic rock fragments that are more common toward the north side of the scarp.

The deposit at the extreme distal part of the inactive landslide along the Lake Fork contains buried wood that provides an estimate of the age of blockage and creation of Lake San Cristobal. Using results of radiocarbon measurements, Madole (1996) estimated the blockage at 800 to 900 yr before the present. The radiometric ages of the oldest deposits described above and the deposits that caused blockage of the Lake Fork could be interpreted as a result of two events separated in time by 100-500 yr. Differences in degree of soil formation on deposits at the distal end at the Lake Fork and the blockage of Slumgullion Creek suggest a period of inactivity (Madole, 1996). However, the distance between the deposit that blocked Slumgullion Creek and the deposit that blocked the Lake Fork is nearly 4 km, and if the landslide were moving at a rate comparable to the current rate, 300 to perhaps 500 yr would be required for the landslide to advance over that distance. Thus, the idea that the landslide activity may be divisible into separate episodes may not be correct. Rather, the sequence we recognize may have occurred as a continuum for perhaps the past 1,300 yr.

The current active movement of the Slumgullion landslide is due to collapse of the north part of the headscarp; movement from that scarp was toward the south. Remnants of the toe of this collapse are preserved in the upper part of the active landslide between elevations 11,200 and 11,400 ft (3,677 and 3,743 m). The exposed materials in the north part of the headscarp are distinctly less weathered (more gray) and less altered than in the scarp farther to the south. The deposits from the collapse cut across features from the earlier collapse of the south part of the scarp, which moved toward the west.

The part of the Slumgullion landslide that was active at the time of our mapping had its upper part, or head, in deposits from the collapse of the north end of the headscarp (sheet 1). The collapse triggered a reactivation of older landslide deposits and propagated movement 2.6 km downslope to about elevation 10,000 ft (3,283 m). There, an active toe apparently formed and emerging landslide material slid over the surface of the old landslide to its current position (sheet 3). The formation and displacement of the active toe were discussed by Guzzi and Parise (1992). Crandell and Varnes (1961) suggested that, on the basis of tree-ring studies, the age of the currently active landslide is about 300 yr. Historical descriptions of the landslide extend from the late 1800's (Endlich, 1876), and the landslide has apparently been moving at a nearly constant rate since then.

TYPES OF MOVEMENT

Actively moving landslides are characterized by fractures and other deformational features that are a result of differential movement at the surface and subsurface. These features collectively determine the kinematics of the landslide. Parts of a landslide having different kinematic expression are separable as **landslide elements**. If a landslide were displaced as a rigid block, there would be a separation between the sliding block and nonmoving material at the head, an area at the toe where the sliding block overrides nonmoving material, and strike-slip faults on the flanks. Because the block is rigid, there would be no fractures within the sliding block.

Most landslides do not behave as rigid blocks. For most landslides, irregular boundaries, different internal forces (driving and resisting), and the deformable nature of landslide materials lead to deformation within the landslide. Certain types of features, as well as their positions and orientations, are typical of different kinds of deformation. Mapping the positions, orientations, and sense of deformation of these features describes the kinematic behavior of the landslide (Fleming and Johnson, 1989; Baum and Fleming, 1991; Baum and others, 1989).

In the upper part of an active landslide, ground that is moving downslope is separating from non-moving ground farther upslope. The features produced are caused by stretching and thinning of the ground in the upper part of the slide as well as in ground uphill from the slide. The most common fractures include tension cracks having their long axes oriented at right angles to the direction of movement and normal faults. In the lower part of a landslide, where the toe is resisting sliding, principal deformation is shortening and thickening. Features such as thrust faults and small buckle folds are typical. Tension cracks are generally oriented parallel to the direction of movement where deformation is simply shortening; the tension cracks may be at right angles to the direction of movement if they form along the crest of a shortening structure such as a buckle fold.

Measurement of displacement at different points across the surface of a landslide produces independent data on deformational features (Fleming and others, 1993). Displacement-rate values should progressively increase from the crown of the landslide to a maximum value at some point that is part way down the surface of a landslide. There, displacement rate should begin to decrease. Along the longitudinal axis of the landslide, increasing displacement rate in a downslope direction indicates stretching and decreasing rate indicates shortening.

On the landslide flanks, strike-slip deformation is predominant. The features along landslide flanks are typically more complex than at the head or toe (see Fleming and Johnson, 1989). The simplest structure on a landslide flank is a strike-slip **fault** where slip occurs across a single surface that is oriented parallel to the direction of slip. A fault segment is similar to a fault in that it is a single surface of slip but is different in that the orientation is misaligned with respect to the overall direction of slip. **Fault segments** are typically oriented 10°-20° clockwise with respect to the slip direction for right-lateral slip and 10°-20° counterclockwise for left-lateral slip (Gilbert, 1928; Fleming and Johnson, 1989). Even though they are misaligned, we know that the segments are faults because their surfaces are smooth and slickensided. Continued displacement on the fault segments causes buckles or small thrust faults to form between the overlapping ends of the fault segments. The **fault zone** is the width of the misaligned fault segments measured normal to the overall trend of the zone.

Tension cracks may also be indicators of strike-slip deformation. En echelon tension cracks are as much as several meters long and inclined from about 30° to 45° clockwise with respect to right-lateral faulting and from 30° to 45° counterclockwise with respect to left-lateral faulting. We know that these cracks originated in tension because they have rough surfaces that would be interlocked if they were closed.

These deformational indicators of strike-slip faulting on landslide flanks may occur separately or together in a zone of shearing. The fracture type that forms is partly dependent on the rheology of the materials at the surface of the landslide. Hard, brittle surfaces tend to fracture as en echelon tension cracks. Very soft, deformable clay tends to produce a simple, throughgoing fault. Materials having properties intermediate between these extremes tend to produce fault segments in strike-slip fault zones.

The simple indicators of strike-slip deformation on the lateral boundary of a landslide become more complex where the fault curves or steps. A left step or bend in a right-lateral fault zone is constraining and contains deformational features characteristic of compression in addition to the lateral shift. A right step or bend in a right-lateral fault zone is extensional and contains deformational features characteristic of stretching. Constraining steps tend to narrow the width of the landslide; extensional steps tend to widen the landslide. Features associated with both narrowing and widening of a landslide are described in Fleming and Johnson (1989).

In addition to fractures that provide a direct indicator of landslide kinematics, trees and tree roots are indirect indicators. In the Slumgullion landslide, trees may be tilted and (or) split; tree roots may be stretched or buckled.

Trees are tilted in active landslides by movement over an irregular failure surface (fig. 3) and by deformation caused by differential rates of displacement. A tree that is undisturbed tends to grow vertically. Tilt of a tree produces new vertical growth at the tip, and the tree develops a kink or curve in the trunk with continued growth. New vertical growth at the tips of tilted trees was used by Fleming and Johnson (1989) to show that a long, linear ridge on the Twin Lake landslide, Utah, was actively enlarging. Tilted trees were used by Fleming and others (1988) to estimate the shape of the failure surface of a slump in the crown of the Manti landslide and by Baum and others (1993) to evaluate a bump in the failure surface of the Aspen Grove landslide, Utah.

The trees on the Slumgullion landslide reflect a long history of movement. Some trees have several distinct bends produced by tilting in different
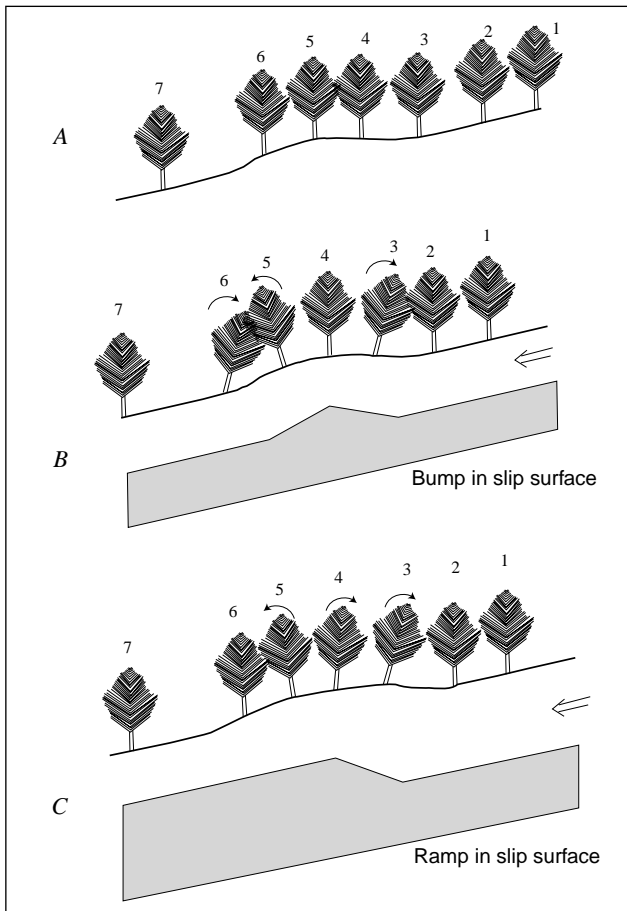
Figure 3. Typical deformation to trees in two different kinematic settings on landslide surface. Measurements of change in orientation of tilted trees can provide information on shape of buried failure surface. *A,* Initial condition of upright trees. *B,* Pattern of tilted trees created by landslide movement over a bump in slip surface. *C,* Pattern of tilted trees created by landslide movement over a ramp in slip surface. Amount of displacement is given by length of arrow and by change in position of numbered trees in *B* and *C* compared to *A.* (From an unpublished figure provided by A.M. Johnson.)

directions as they were transported downslope by sliding. On the map of the Slumgullion landslide, we use two types of information from trees. First, there are several places where trees have been split by differential displacement across a fracture. The direction of differential movement required to produce the split is used as an indicator of local deformation. Likewise, the local deformation is indicated in the direction of stretching or buckling of tree roots.

In summary, deformational indicators identify the kinematics of different parts of an active landslide. Generally, the head of a landslide is characterized by stretching and thinning, the toe by

shortening and thickening. The flanks contain indicators of strike-slip deformation that may be faults, fault segments, or tension cracks where the zone is simple. Fracture patterns become more complex where landslide boundaries are irregular. Compressional or extensional bends occur where the landslide becomes narrower or wider, respectively. Some of the bends are in the form of steps, others simply involve a curving fault zone. We use fracture patterns together with indirect information from split trees, tilted trees, and stretched tree roots to infer the kinematics of the active part of the Slumgullion landslide.

THE LANDSLIDE

MAIN HEADSCARP

The headscarp of the Slumgullion landslide is nearly 1.3 km long and has a maximum height of about 200 m (elevation 3,500-3,700 m); part of the north part of the scarp is shown on sheet 1. The overall trend of the scarp is about northwest-southeast. The older part of the scarp, the southeast end, contains an abundance of hydrothermally altered material that matches much of the general appearance of the materials in the landslide. Yellow, white, gray, and red silty clays form smooth, rounded hummocks on the unvegetated lower part of the scarp. The upper part of the scarp is tree covered and may be underlain by less altered rocks (Diehl and Schuster, 1996). The average slope of this part of the scarp is about 75 percent (35°-40°). From near the southeast end for about 700 m, the scarp apparently formed by breaking through the crest of Mesa Seco, and the top of the scarp is a local topographic divide. The northwestern part of the scarp is formed in more resistant rocks and is steeper than the southeastern part, the slope being nearly vertical in places.

The materials exposed in the main headscarp are a complex array of hydrothermally altered and unaltered volcanic materials including tuffs and intrusive and extrusive rocks of variable composition (Diehl and Schuster, 1996). The Miocene Hinsdale Formation at the top of the scarp is unaltered vesicular basalt. Below the basalt is the Miocene Sunshine Peak Tuff, a welded ash flow tuff. These Miocene units unconformably overlie the highly altered Oligocene volcanics of Uncompahgre Peak, which consist mainly of andesite flows (Lipman, 1976). The products of hydrothermal alteration, including alunite, smectite, and opal, have been found in the altered rocks of the main scarp as

9

well as in the debris forming the slide (Larsen, 1913; Diehl and Schuster, 1996). Faults, breccia pipes, jointing, and alteration contribute to the instability of the main scarp, and rock avalanche chutes coincide with many of the faults (Diehl and Schuster, 1996).

ACTIVE LANDSLIDE

This description of the active part of the Slumgullion landslide begins at the head and proceeds downslope to the toe. The flanks of the landslide are defined as looking downslope as the left or right flank; at Slumgullion, the left flank is the south side and the right flank the north side of the landslide. The active landslide can be divided into seven zones based on similarity of structural features within each part. The uppermost, zone 1, is called the **head.** It contains fractures indicating both stretching and shortening. Downslope from the head is zone 2, a **broad zone of normal faults and tension cracks** that is more than 350 m wide. Zone 3, the **hopper and neck**, is a funnel-shaped stretch where the landslide width is at its minimum and the displacement rate at its maximum. Downhill from the hopper and neck, the landslide gradually increases in width through curves in the flank faults, creating zone 4, an area of **pull-apart basins** along both flanks. Zone 5 is an area of **pond deposits and the emergent toe**, followed by zone 6, an **area of shortening and spreading**, and zone 7, the **active toe**.

For each of the seven zones, we include an interpretive cartoon drawing (figs. 4-8, 10, 11) showing some of the main structural features in that part of the landslide. Alphabetically noted points have been added to both sides of the cartoon so that the reader can readily locate the part of the landslide being described. The cartoons contain a small area of overlap with adjacent zones. In these overlap areas, not all the schematic fractures are shown unless they are within the zone under discussion. The reader may find it helpful to first locate features on the cartoon before attempting to locate them on the larger, more detailed maps.

Zone 1—Head

The uppermost fractures that we mapped in the head of the landslide form a 150-m-wide zone on a topographic bench below a large pile of coarse talus (fig. 5, sheet 1). The fractures are tension cracks and normal faults, both indicating stretching. The landslide material in the area of the fractures is a powdery clayey silt to silty clay that does not preserve fractures well. The scarps of the normal faults are

0.1-0.2 m high. Some face uphill, others downhill. Several features that have the appearance of sinkholes and long, linear furrows are interpreted to be depressions above tension cracks that opened at depth and propagated to the surface as collapse features. The band of most active fractures, near *A-A'*, is about 100 m across the landslide and about 20 m wide in the direction of sliding. The stretching rate across the zone of fractures is about 0.2 m/yr. The flanks of the landslide downhill from this zone of stretching are obscure, but several segments of an active strike-slip fault are preserved along the left flank about 70 m downhill. Other than these few faults, the flanks were located (fig. 4, sheet 1) by an abrupt change in slope or a small furrow. Movement rates apparently are insufficient to maintain a conspicuous set of fractures in this area.

The direction of sliding at the head is toward the south and is in the same direction as the inferred collapse of Mesa Seco (fig. 2*A*). Remnants of the toe of this collapse are preserved as linear ridges outside the left flank in the vicinity of *C'* and within the active landslide along a discontinuous zone of toes about 70-90 m downhill from the line *C-C'*. Uphill from the toes, in the area of *C-C'*, is another zone of stretch features much like the uppermost zone mapped at *A-A'* and consisting mostly of uphill-facing scarps as much as 1.5 m high.

The stretch (lengthening) features produced by normal faults and tension cracks in the active landslide contrast sharply with the compressional (shortening) features produced by collapse of part of the main scarp in the same general area. The uppermost stretch features are at *A-A'*. Principal shortening features are along a line between *D* and *C'*. Here, a zone of discontinuous internal toes and trees that have been pushed over and partly overridden by landslide material are diagnostic of shortening. Overlapping the shortening features is a band of stretching features, principally scarps of normal and oblique-slip faults, that loosely connect with the north (right) flank. The stretch faults are probably a continuation of the zone of normal faults that intersect the right flank between *D* and *E*. The toe of the small landslide between *A-A'* and *D-C'* is being pulled apart by more rapid movement along the right flank farther downhill.

Displacement rates in the head of the landslide are about 0.2 m/yr southward. The movement in the head of the landslide is nearly independent of the westward movement farther downslope. The value of 0.2 m/yr at the uppermost fractures is minimal because measurement points did not extend

SLUMGULLION LANDSLIDE

Head

Zone 1

Toe

0   500

Scale (m)

N

N

× A'

A
+

0.2

B'
+

B
×

0.3

0.4

Left flank

Right flank

C
×

D
×

0.3

0.1

0.5

C'
+

E
×

0.3

0.1

EXPLANATION

Fracture—Dotted where inferred

En echelon fractures—Indicate strike-slip faulting

Scarp—Hachures face same direction as scarp

Thrust fault—Sawteeth on overriding block

0.3 Arrow showing direction of lateral shift across fault zone—
      Displacement in m/yr

A'   Reference point for features described in text

0.3 Arrow showing direction and amount of movement for a point
      within the active landslide—Displacement in m/yr.
      Data from aerial photographs taken in 1985 and 1990

0   100   200

Scale (m)
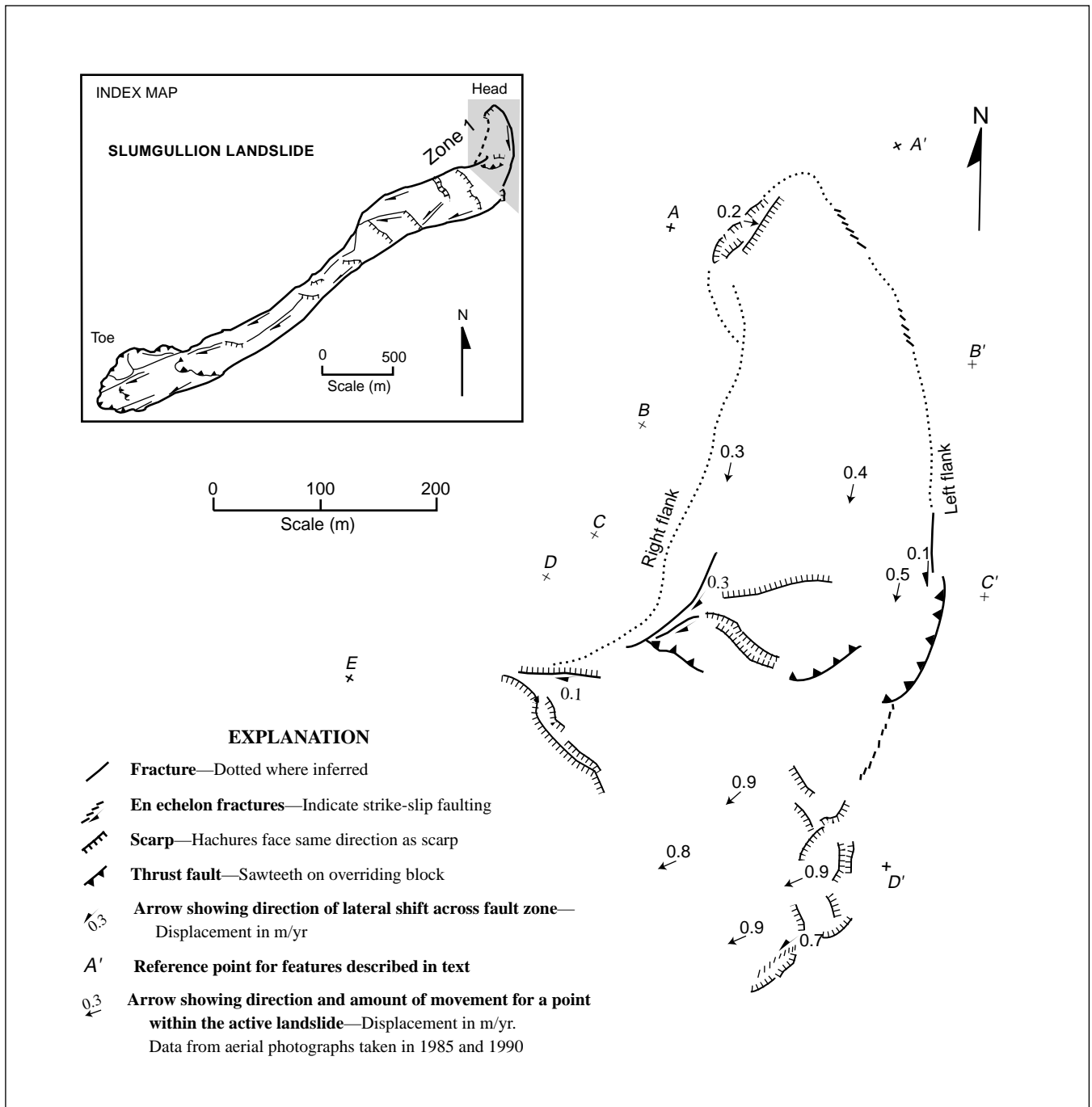
0.9

0.8

0.9

+
D'

0.9   0.7

Figure 4. Simplified interpretive map of deformational features in zone 1, head.
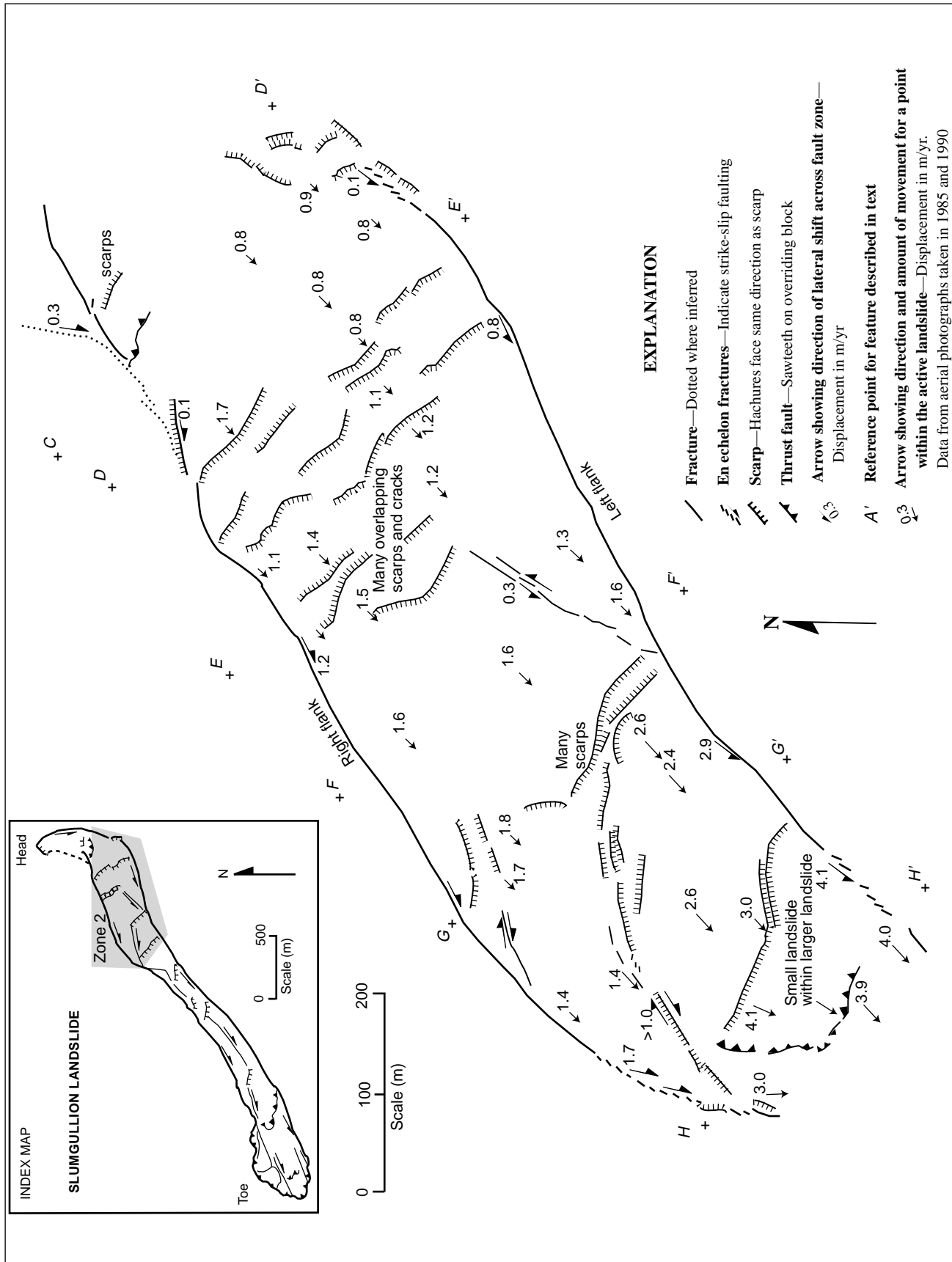
Figure 5. Simplified interpretive map of deformational features in zone 2, broad bands of normal faults and tension cracks.

across all the fractures. Farther downslope, at a point on the left flank about 25 m uphill from line C-C', movement was only 0.1 m/yr. On the right flank, a point near line C-D' was displaced 0.3 m and a point 110 m downhill from there and due south of D was displaced 0.1 m/yr. These few measurements indicate the displacement pattern in zone 1, the head, is largely from a separate, discrete landslide that resulted from the collapse of the north side of the main scarp. Indeed, we were unable to find continuous fracturing along the left or right flank directly uphill from D-D', and the interior of the landslide in the vicinity of D-D' has very few fractures of any type that would connect the small landslide between A-A' and D-C' with the larger active landslide farther downslope.

Zone 2—Broad Bands of Normal Faults and Tension Cracks

Fracturing that is more nearly typical of that in the head of a landslide is found in three broad bands of normal faults and tension cracks within zone 2 (fig. 5, sheet 1). Overall, the zone is nearly 1,000 m long and as much as 350 m wide. Fractures are similar in each of the bands; they reflect stretching or extension. Included are normal faults with scarps facing both uphill and downhill, tension cracks oriented approximately at right angles to the direction of sliding, and stretched roots and split trees showing the stretch direction parallel to the direction of sliding. The main structures and annual displacement for a few points within and on the boundaries of the landslide are summarized in figure 5. Displacement progressively increases through the zone of stretching from less than 0.1 m/yr to more than 3 m/yr over the length of the zone.

The uppermost band of stretching features, which intersects the flank near point C on the north side of the landslide, contains normal faults in a 200–m-long band that extends only part way across the landslide at C-D' (fig. 4). This band extends through the thrusts of the landslide deposit in zone 1. It occurs at the abrupt 90° clockwise bend in the landslide and contains a right-lateral, strike-slip fault on the north side that carries almost the entire displacement on the right flank (fig. 5). The strike-slip fault is loosely connected with the poorly developed normal faults and tension cracks that extend part way across the landslide. Boundary fractures farther to the north appear to be inactive, or the landslide is moving too slowly there to maintain open fractures.

Displacement rates are 0.3 and 0.7 m/yr on the north and south sides of the landslide, respectively. If the movement was purely rotational, we would expect the velocities to be about 0.3 m/yr on the north and 0.72 m/yr to perhaps as large as 0.85 m/yr on the south side of the bend. Thus, the slide mass in this area is essentially rotating (plan view) through the 90° bend as a rigid body.

The middle band of stretching extends across a broad area between E and E' (fig. 5). This band extends entirely across the 350-m-wide landslide and downhill at least 250 m. Individual scarps do not extend all the way across the landslide; rather, they occupy the band as many overlapping normal faults and tension cracks. Scarps of the active normal faults range to as much as about 2 m in height. Inactive scarp heights locally exceed 5 m.

The band of structures at E-E' reflects stretching in this area, which produces an increase of sliding rate. On the left flank, the sliding rate increases from 0.8 m/yr near E' to 1.4 m/yr near F'. On the right flank, the sliding rate increases from 0.1 m/yr near D to 1.2 m/yr between E and F.

The difference of 0.4 m/yr in displacement rate on the right flank at E compared to the left flank of the landslide at E' (1.2 m/yr compared to 0.8 m/yr) has kinematic significance. The difference must be accommodated either by internal distortion or by movement on one or more fault zones within the body of the landslide.

As we have proceeded down the landslide, we have seen two ways that the velocity changes are accommodated. One is normal faulting and tension cracking that reflects an increase of sliding velocity first across the bend and then near sections E-E' and F-F' within the landslide. We also saw rigid block rotation at D-D'.

A different form of accommodation is visible at F-F'. Here, displacement rates are larger, and the landslide does not move through the curve in the boundaries by block rotation. The normal faults and tension cracks of zone 2 terminate in a left-lateral strike-slip fault zone (near the left flank at F' and trending from F' toward D, fig. 5) that carries about 0.3 m of the displacement rate difference between the landslide flanks. The internal left-lateral fault near F' bounds a block that moves through a 20° bend between F' and G' with relatively little internal distortion because the block is free to move nearly parallel to the flanks downhill from the bend.

Continuing downslope, a third band of normal faults (fig. 5) extends from F toward H. Here, scarps

and fractures are in a band more than 50 m wide that turns and transforms into a right-lateral strike-slip fault where the band narrows midway across the slide near *G*. The right-lateral strike-slip fault intersects the right flank near *H* (fig. 5). The displacement rate along the right flank is 1.8 m/yr near *G* and declines to 1.7 m/yr near *H*. The displacement rate along the left flank increases from 2.9 m/yr near *G'* to 4.1 m/yr near *H'*. Thus, there appears to be a displacement rate of at least 1.1 m/yr across the internal right-lateral strike-slip fault. The position of this band also corresponds to a sharp bend in the right flank of the landslide; it turns counterclockwise 30° directly upslope from *H*. The left flank, though, is relatively straight. The area along the right flank between *G* and *H* was recognized as a relatively "dead zone" by Guzzi and Parise (1992) because of the minor amount of internal deformation there.

Another band of normal faults beginning at *H-H'* (fig. 6) extends across most of the width of the landslide. This group of faults gives the appearance of an additional zone of stretching. However, a belt of thrust faults (internal toes) just downhill from the scarps reveals that this structure is a small landslide superimposed on the larger landslide in a region of steeper slope (fig. 6, sheet 1).

Within zone 2 we recognize three different structures in the region of stretching, two of which are a result of curving boundaries and one of which results from simple stretching. The clockwise bend (fig. 4) between *C-D* and *C'-D'* is an area of rigid-block rotation. The area beginning at *D-E'* (fig. 5) and continuing downslope for 200 m is simple stretching across normal faults and tension cracks. Here the flanks of the landslide are relatively straight and parallel across this zone. The landslide accommodates bends at *G-G'* and *H-H'* with internal strike-slip faults that contain most of the slip difference between the amounts on the landslide flanks. Both of the broad bands of normal faults have an associated strike-slip fault that joins the band to the flank where it curves (fig. 5). The strike-slip faults allow internal blocks to slide with very little internal deformation of the slide material between the faults.

On the basis of our mapping across the zone of stretching, we can make the following important observations:

I.   The landslide moves as a series of blocks bounded by zones of deformation. The deformation within blocks is very small.

II.   Accommodation between blocks occurs by formation of multiple discontinuities in the form of faults and other structures that accommodate highly localized deformation.
III. The two primary modes of movement of blocks are plan-view rotation and translation.

From the downhill end of zone 2 the appearance of the landslide changes dramatically. Gone are the scarps and other stretching features that extend across the landslide. These are replaced by scarps that are oblique or longitudinal with respect to the landslide boundaries, and different kinds of structures are produced.

Zone 3—The Hopper and Neck

The hopper is a 200-m-long, funnel-shaped area in the 400-m-long zone termed "hopper and neck" that accommodates narrowing of the landslide (fig. 6, sheets 1 and 2). The right flank of the landslide has a major restraining bend while the left flank is very straight. The width of the landslide decreases from 230 m at *H-H'* to 180 m at *I-I'*, over a horizontal distance of 150 m.

The hopper begins where there is an abrupt increase in slope and extends downslope to the narrowest part of the landslide, the neck. The materials entering this narrowing part of the landslide are constrained laterally, and materials have the appearance of entering a hopper.

On both sides of the landslide, 30-50 m downhill from point *H*, the landslide surface has been tilted toward the center (indicated by "tilt" with arrows on fig. 6). The tilting extends a little farther downslope on the south side. The slope of the tilted surface on the north side is as much as 50 percent whereas the slope of the tilted surface on the south side is less, as much as 20 percent. The downslope end of the tilted surface on the north side is terminated by a discontinuous line of scarps that extends from the north flank near point *H*, obliquely toward point *I'*. The sense of slip is oblique containing both left-lateral and normal movement. Small en echelon tension cracks in the line of scarps provide the basis for kinematic interpretations.

The inferred deformation within the hopper is depicted in two idealized cross sections across the landslide (fig. 7). Trees on the tilted surface on the side near *A* and *B* (fig. 7) are uniformly inclined toward the middle of the landslide and are tilted approximately normal to the ground surface. Trees are generally absent on the south side of the hopper.
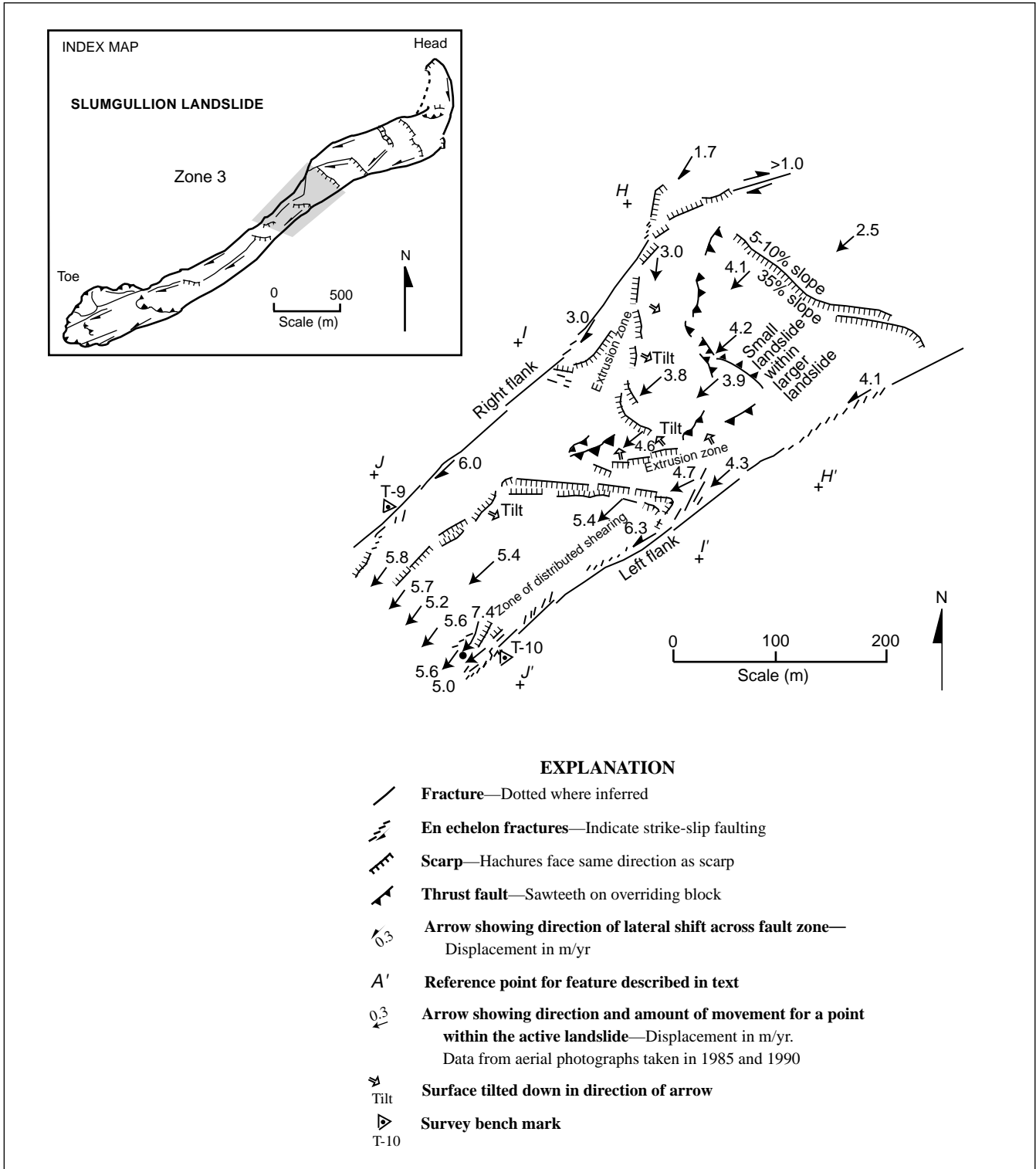
14

Figure 6. Simplified interpretive map of deformational features in zone 3, hopper and neck.

15

The tilted surfaces are inclined toward each other, and the trends of the inclined surfaces form an asymmetrical V with an intersection point near the middle of the landslide at *I-I'* (fig. 6). Along both flanks of the landslide, from *H* to *I* and *H'* to *I'* (fig. 6), the landslide debris is devoid of trees and soft, powdery, white-to-yellow, clay-rich material is exposed. The remaining trees on the surface of the landslide between points *H* and *I* are along the bottom of a swale that trends down the middle of the landslide. Idealized motion on each flank of the hopper appears to be screw-like (in transverse cross section) with material being extruded near the landslide flanks and being folded together along the midline of the landslide (fig. 7). Landslide materials are extensively remolded in the short stretch between *H-H'* and *I-I'*. The hopper-like structure ends approximately at *I-I'* where two thrust faults having traces oriented parallel to the direction of sliding mark the intersection of the tilted surfaces.

The downslope end of the hopper structure is abruptly broken by a belt of normal faults and tension cracks. The belt begins with a chevron-shaped scarp near point *I'*. Small en echelon tension cracks in the west-trending zone about 50 m inside the south boundary at point *I'* indicate that slip is oblique, right-lateral, and normal (down). Most of the narrowing of the landslide has been accommodated farther upslope, and this structure is apparently formed to accommodate stretching. Maximum displacement rate is near the line *J-J'*.

A line of fractures and scarps trends downslope from the end of the chevron-shaped zone of normal faults (halfway between points *I* and *J*, 50 m inside the north boundary). This line continues downslope about parallel to the landslide boundaries. The features along the line are not well preserved; locally, there are en echelon cracks indicating that the zone is partly a right-lateral strike-slip fault. Definitive evidence from split trees or stretched roots is lacking, though. The zone may be a relict structure that was produced in the hopper and has been transported downhill. As such, it would have limited kinematic significance for current movement. On the other hand, there is a well-developed, longitudinal, right-lateral fault zone farther downslope that may carry as much as 0.5 m/yr of differential displacement (fig. 8). These longitudinal fractures in the neck could be the beginning of that fault zone.

The landslide continues to narrow to near the line of *J-J'*, where it is about 160 m wide. Maximum displacement rate was recognized by Crandell and Varnes (1961) to be near here, and they established a

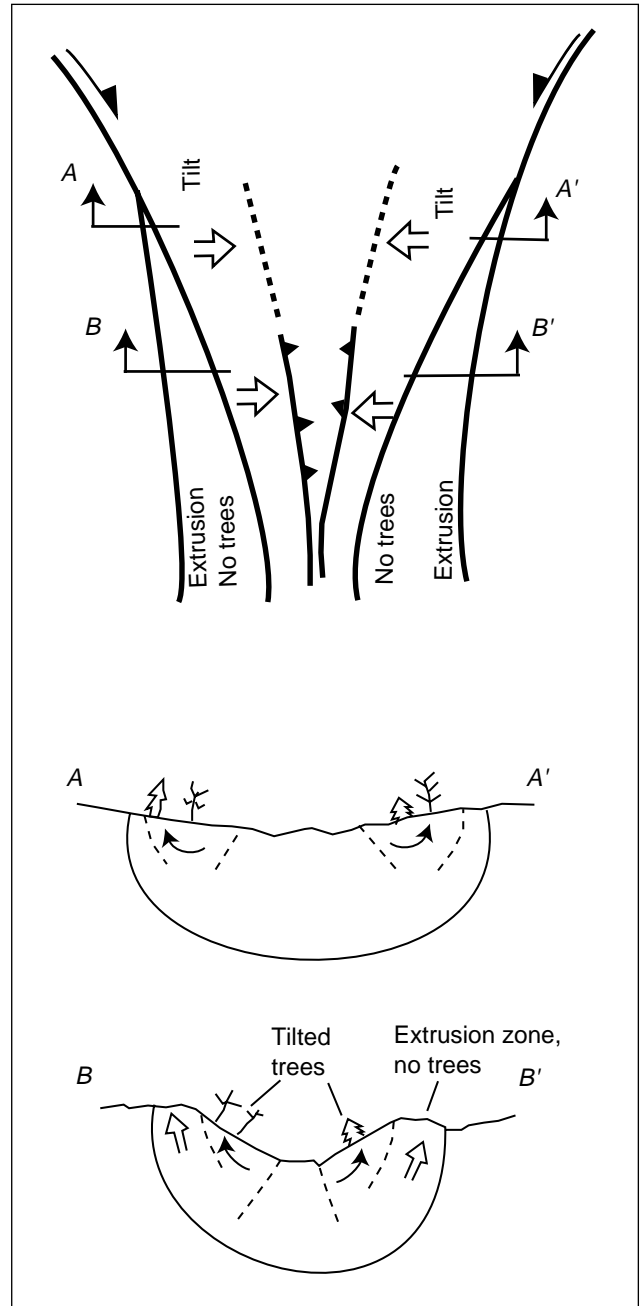**Figure 7.** Cartoon of an idealized plan view and cross sections through two places in the hopper. As the ground surface is tilted toward middle of the hopper, fresh material is extruded onto ground surface between landslide flanks and edges of tilted blocks. Width of extrusion deposits increases downslope. The two thrust faults shown trending down the axis of the landslide on the plan view represent shortening and compression.

survey line and took time-lapse photographs of the movement. Note that there is a poorly developed right-lateral fault about 30 m from the south boundary at **T-10**. This fault is apparently the right side of a small landslide element along the south flank that is superimposed on the larger Slumgullion landslide. Displacement rate should be a maximum here where the shallow movement is superimposed on the maximum rate of displacement of the Slumgullion landslide. The point having the value 7.4, shown at the bottom of figure 6, is believed to be near the point of maximum rate. This value was from a spot measurement and may not be a credible representative of displacement rate over a longer period of time. Near the point of the spot measurement, a line of six rebar rods was surveyed several times over a 4-yr period. Movement rates of individual rods ranged from 5.2 to 5.8 m/yr in the main body of the landslide and are probably a better indicator of maximum landslide velocity (fig. 6).

There are extensive fractures along the strike-slip zone of the left flank in the neck area. These fractures are inclined at 30°-50° counterclockwise to the main strike-slip fault zone on the boundary; some of the fractures have a low, downhill-facing scarp but most appear to be tension fractures. The fractures make up a zone 5 to 10 m wide and, overall, appear to define a broad zone of left-lateral shearing adjacent to the left flank (identified as distributed shearing on fig. 6, mapped on sheet 2). In most places along the landslide flanks, shearing is confined to a zone that is less than a meter wide.

The upper part of the landslide was dominated by movement of large blocks bounded by zones of intense deformation. That behavior contrasts markedly with movement in the hopper and neck, where materials are intensely deformed throughout. Downhill from the hopper the landslide behavior partly returns to movement of blocks bounded by zones of intense deformation, partly to flow-like structures, and partly to development of structures indicative of a decreasing displacement rate.

Zone 4—Pull-Apart Basins Along Both Flanks[2]

The landslide widens downhill from the neck at steps or offsets in both flanks (zone 4, fig. 8, sheet 2). Over a distance of nearly 1 km, the slide widens from 160 to 260 m. Over this same distance, the dis-

placement rate declines from about 6 to 4 m/yr . Long, narrow pull-apart basins[2] have formed directly downhill from three right-stepping offsets in the right flank and at one small, left-stepping offset in the left flank (fig. 9). A step in the bounding flank fault forms at a bend in the fault that tends to widen the landslide (clockwise bend on the right flank, counterclockwise bend on the left flank). Within a few meters downhill of the bend, a topographic depression forms between the flank fault and the projection of trend of the fault from uphill of the bend. The landslide material deforms to fill the basin, and the basin is filled over a distance of several hundred meters. Part of the deformation is by the movement of blocks and part is by flow-like deformation. The best expressed basin is on the north side, between points *J* and *K* (fig. 10).

The zone of strike-slip faulting on the north (right) flank bifurcates where it changes orientation at point *J* (fig. 10). One part follows the north flank as a narrow zone of strike-slip faulting on the landslide boundary; the other part forms a crescent-shaped group of scarps and fractures that gradually turns parallel to the north flank. A 5-m-deep basin occupies the area between this crescent-shaped group of scarps and the north flank. Within the basin and parallel to the landslide boundary are several shortening features, such as small thrust faults and buckle folds. Rotated blocks bounded by the crescent-shaped group of scarps and the shortening features in the basin are smaller landslides within the overall larger landslide in which material is being transported obliquely into the basin (fig. 10). The crescent-shaped group of scarps is the surface manifestation of oblique-slip (right-lateral- and dip-slip) listric faults. The structure appears analogous to pull-apart basins in larger tectonic settings where movement on listric faults transports material from the flanks of the basin to its center.

About 200 m downhill from point *J*, the group of crescent-shaped scarps turns toward the basin and terminates in the basin in folds and thrust faults (fig. 10). The buckling and thrusting is evident mostly in the tilting of small trees and bushes toward the deepest part of the basin. Individual faults are difficult to recognize, so that the deformation resembles flow rather than block deformation. There is a small pond at the deepest part of the basin that accumulates water-transported sediment that helps fill the basin. Pond sediments extend downslope from the existing pond as the landslide translates the materials. The pull-apart structure, though, stays in the same place.

---

[2]Pull-apart basins are structural and topographic basins that form next to the flanks where they step laterally to widen the landslide (releasing step in a fault zone).

Figure 8. Simplified interpretive map of deformational features in zone 4, pull-apart basins along both flanks.

A

B

Figure 9. Two views of the deepest part of the pull-apart basin looking downhill or westerly. *A*, Pond sediments contribute to filling the deepest part of the basin. Small spruce trees to left of pond are tilted to the right and curved in response to a component of thrusting in that direction. The jumbled aspen trees in the right foreground are the result of a component of movement from left to right along an oblique-slip fault. *B*, Closer view of pond and pond sediments in the deepest part of the basin. The bounding flank fault is visible in the small troughs to the left of and downhill from the tripod. The dark-colored material in the left foreground that is surrounded by pond sediments is a compressional structure produced by a component of movement into the basin. Overall displacement rate at this part of the landslide is about 4 m/yr. The deformational features within the pull-apart basin are the result of a small component of the overall displacement rate.

19

Downhill 50 m from point *K* (fig. 10), the basin has been completely filled. Farther downhill from the basin there are numerous inactive scarps and hummocky topography, shown on the sketch (fig. 8) as "hummocky ground." These inactive features apparently formed in the pull-apart basin and were deactivated as they were transported beyond the basin.

Other basins along the active flanks of the Slumgullion landslide (fig. 8) do not contain all the features shown in figure 10. However, they do generally have slump blocks that are moving from the inboard side of the basin toward the flanks. The toes of these slumps form compressional features including folds and thrust faults in the deepest parts of the basins.

A discontinuous line of scarps that begins in the middle of the landslide at *K-K'* trends axially to about 150 m uphill from *M-M'*. These scarps are along a zone of right-lateral shear that apparently contains about 0.5 m/yr of displacement. The south side of the landslide is moving 0.5-0.8 m/yr faster than the north side.

There is one puzzling structure in this zone (fig. 8). A narrow zone of scarps and tension cracks trends partway across the slide from about point *M* toward *M'*. This zone generally follows a line of abrupt increase in slope. The position of this zone is perhaps 100 m downhill from the inferred position of the buried drainage divide separating the Slumgullion Creek drainage basin on the south from the basin of an unnamed creek to the north. These fractures appear to be superimposed on other fractures associated with a poorly developed pull-apart basin and an axial right-lateral strike-slip fault zone. The scarps and tension cracks are consistent with arching that could occur as landslide debris passes over a buried topographic bump; and, indeed, the structure forms at a sharp break in slope from a bench to a much steeper section. The scarps and cracks could also be due to superficial sliding along the steeper slope just downhill on the active landslide.

Zone 5—Pond Deposits and Emergent Toe

Zone 5 contains an area of thrust faults and extensive pond deposits. The area of thrust faults uphill from the pond deposits is centered approximately on *O-O'* and is the first indication of deep-seated shortening on the landslide (fig. 11, sheet 3). Other thrust faults uphill from this area are related to pull-apart basins or represent internal toes of small landslides superimposed on the larger land-

slide. Across the zone of thrust faults at *O-O'*, the displacement rate diminishes from about 4 m/yr to about 2.5 m/yr. The position of this zone of shortening coincides with a large, inactive segment of landslide toe to the north of the active landslide flank at point *O*. This inactive part of the toe is labeled, but its outline is not shown on the sketch (fig. 11). Even though the toe segment to the north is inactive, it overlies older, inactive deposits of the Slumgullion landslide and is topographically contiguous with the active landslide. Thus, the toe segment is a deposit that formed and became inactive during creation of the current landslide toe. As such, this deposit is less than 300 yr old and overlies landslide deposits that are between 900 and 1,300 yr old.

Pond deposits are recognizable in many places on the active landslide by their uniform tan color and silty texture. About 2.8 km downhill from the active landslide head and about 0.6 km uphill from the front of the active toe, there is an extensive area (80 m by 80 m) of pond deposits (fig. 11). These deposits begin near line *P-P'*, directly downslope from hummocky topography with thrust faults. The area contains a small shallow pond. The surface has been tilted northward to the point that a small stream that formerly fed the pond now flows across the north side of the pond deposits and continues downhill. A few dead and broken spruce trees protrude from the sediment where they were partly buried. Small aspen and spruce trees have sprouted in the pond sediments near the downhill edge of the depression (fig. 12). The downhill edge is at a broad break in slope that separates surfaces that are tilted uphill from those tilted downhill.

The pond sediments extend downslope at least 250 m beyond the edge of the pond as defined by the break in slope (Van Horn, written commun., 1994). Apparently, the location of the pond has remained fixed while the landslide material has been displaced across the pond site. Fixed features have also been observed at other landslides (Fleming and others, 1988; Baum and others, 1993). Given the current rate of movement at the pond site, the position of the pond apparently has remained fixed for about 100 yr and perhaps longer (Van Horn, written commun., 1994).

Parise and Guzzi (1992) suggested that the pond sediments and thrust faults mark the initial position of the toe of the reactivated Slumgullion landslide. Observations at the tip of the currently active toe indicate that it is moving along the surface of the old landslide deposits in bulldozer fashion, toppling and overriding trees as it goes. Upslope of the area
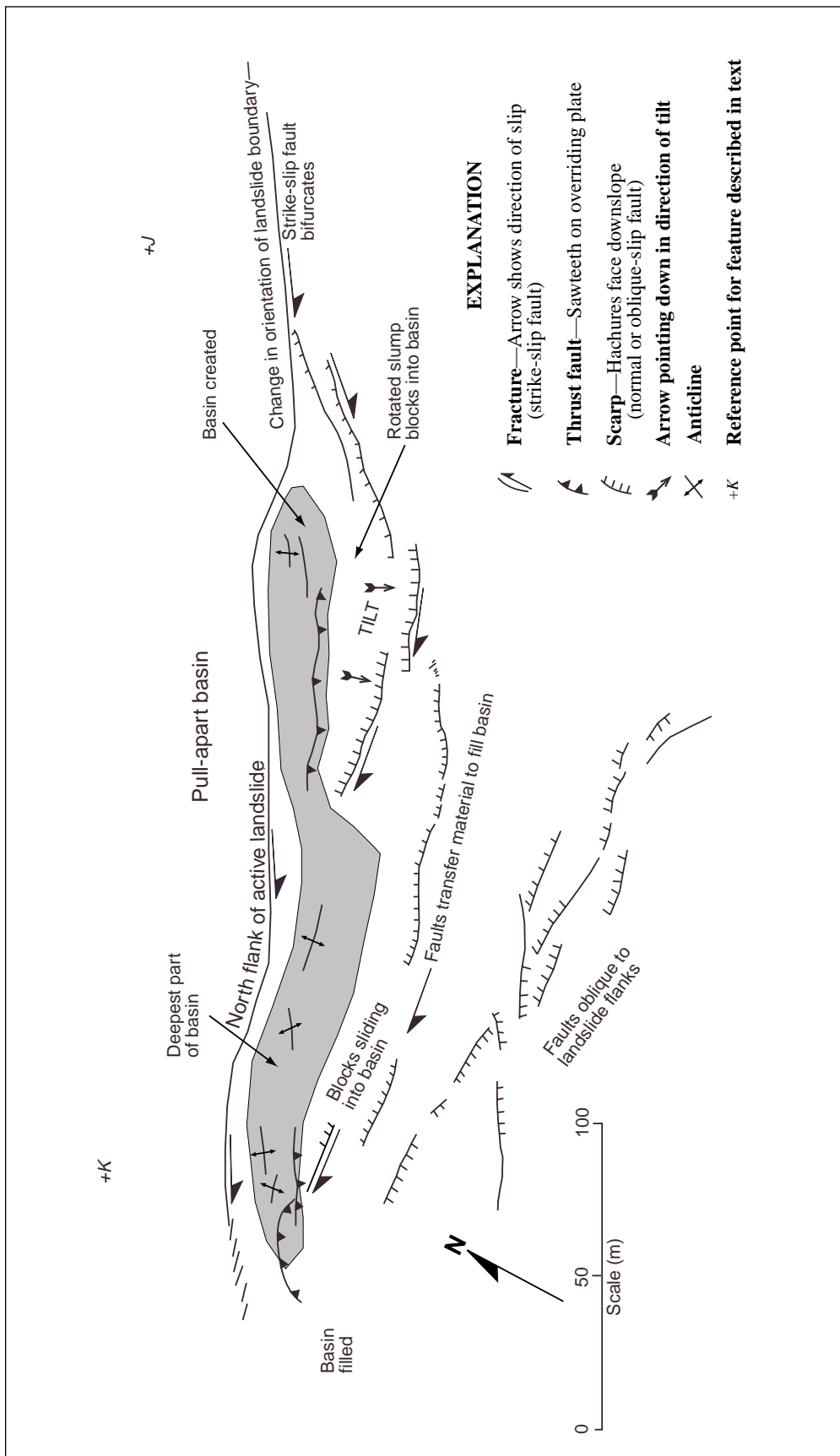
Figure 10. Idealized features in same pull-apart basin as shown in figure 9 (between points J and K). The basin forms where the landslide becomes wider through a bend or step in bounding strike-slip fault. Features created within moving landslide serve to translate material into the basin. In upper part material is moved into the basin by a series of rotational slumps. Farther downslope material is translated into the basin along curving strike-slip faults that terminate in the basin in buckle folds and thrust faults. At downslope end of the basin a zone of oblique slip faults translates material across landslide and completes filling of the basin.
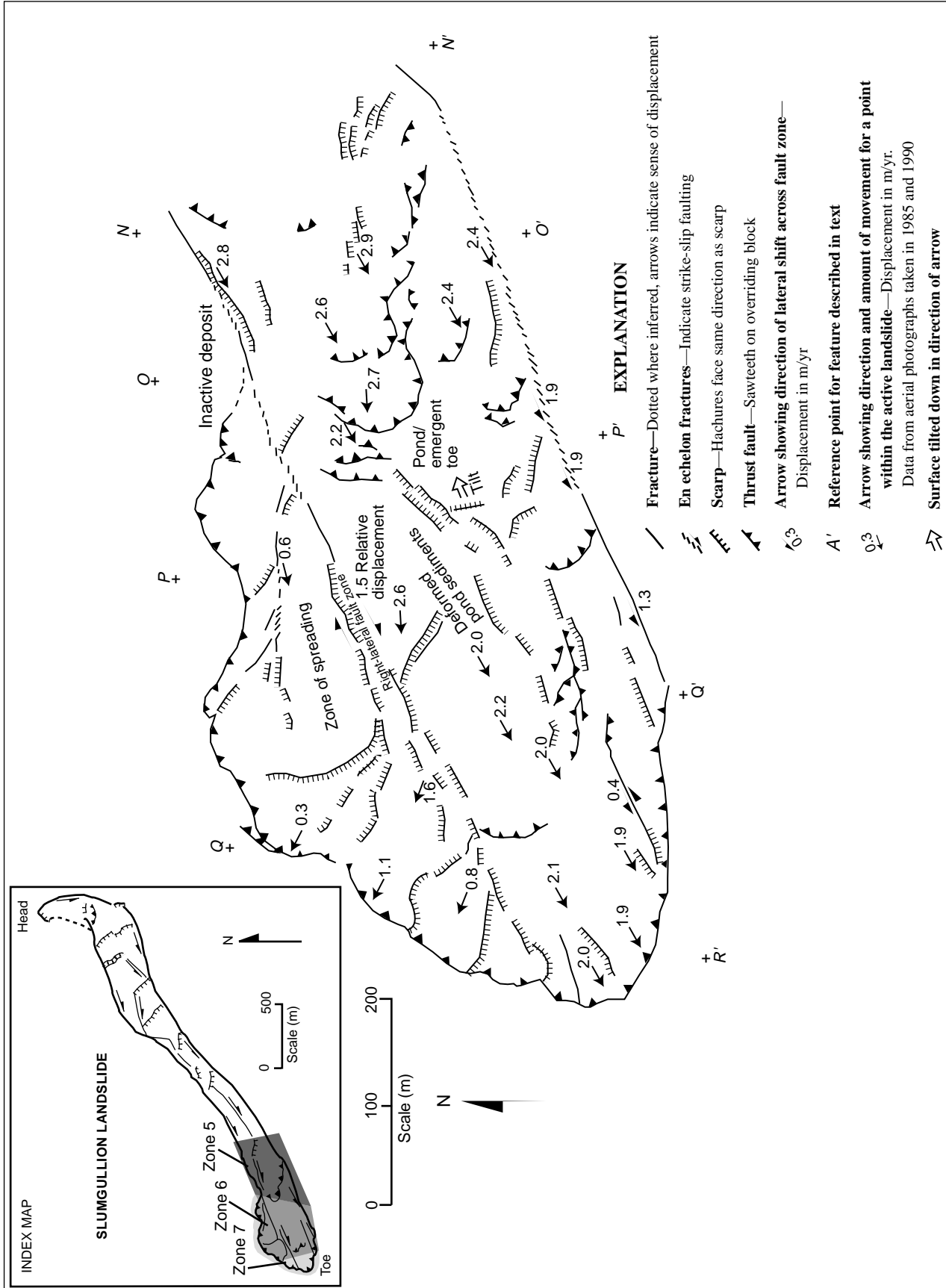
Figure 11. Simplified interpretive map of lower part of the active landslide, zones 5, 6, and 7. Features shown include thrust faults and tension cracks of zone 5 (pond deposits and emergent toe), thrust and oblique-slip faults of zone 6 (region of shortening and spreading), and zone 7 (active toe).

of thrust faults (uphill of *N-N'*), the reactivated landslide appears to be formed **within** the older landslide deposits. At the pond and farther downhill, the reactivated landslide materials are sliding **on top** of the older deposits.

The concept of the processes of formation and preservation of the pond is outlined in figure 13, which is a sketch showing the influence of the shape of the failure surface on the morphology of the landslide. The response to the collapse of the north side of the headscarp and loading in the head of the inactive landslide apparently triggered the reactivation. Fractures propagated downslope through the inactive landslide material to the approximate position of the pond. There, the fracture along the basal failure surface emerged to the ground surface (fig. 13). From this point on, the reactivated landslide advanced over the surface of the old, inactive landslide. While this explanation for the positions of the thrust faults and the pond deposits is consistent with observations, the mechanism has not been documented.

Zone 6—Region of Shortening and Spreading

At *N-N'* (fig. 11) the active landslide is about 260 m wide. Downslope 500 m the landslide is 430 m wide. This increase in width is a result of spreading along the north flank. The zone of spreading on the north side contrasts with a zone of shortening on the south side. The different kinematic expressions of the two parts of the landslide are separated by a major right-lateral strike-slip fault that bounds the north flank of the landslide at point *N* and continues internally through the landslide beginning near point *O* (fig. 11, sheet 3). This major dividing fault intersects the downslope end of the active landslide about 150 m northwest of point *R'*. North of this fault, the landslide is advancing and spreading. South of this fault, the landslide is advancing but at progressively reduced rates because of internal shortening within the landslide.

The deformation structures on the north side of the landslide consist of strike-slip and oblique-slip (right-lateral slip and opening or spreading) faults. Pure strike-slip faults are difficult to identify in this part of the landslide because the crumbly landslide debris does not preserve fractures well. In a few places along the trends of some strike-slip faults, there are scarps that enable the fault positions to be accurately located. Where pure strike-slip faults change orientation a scarp is produced and stretched roots or split trees (fig. 14) show that the fault

Figure 12. View (looking downslope) of pond sediments on back-tilted surface at the location of emergent toe of active landslide. Note young spruce and aspen trees growing along divide at downslope end of pond. Note also that older spruce trees in foreground have been buried by pond sediments. Evidence such as this indicates that location of pond has remained fixed while trees have been transported into pond and beyond.

accommodates oblique slip indicative of spreading of the toe.

The major strike-slip fault bounding the north flank at point *N* divides near point *O* into two parts. One part curves northwesterly (obliquely) down to the active toe. The main fault continues southwesterly to between points *P* and *Q,* where it divides again, here into three parts. In each instance, the curving fault trends toward the landslide boundary and apparently accommodates oblique slip. The spreading is accommodated by these oblique-slip fractures.

The entire north side of the landslide toe is composed of oblique-slip structures. Deformation across these structures consists of right-lateral slip, opening and spreading. This is well illustrated at a spruce tree that was caught in one of these oblique-slip zones (fig. 14). The fault zone occupies a small furrow that crosses under the tree. There are no open cracks or fractures; the position of the fault is given only by the furrow and the split tree. The right-hand side of the tree is about 1 m farther downslope than the left-hand side, and the opening normal to the strike-slip direction is about 0.8 m. The split tree is definitive evidence of right-lateral slip together with spreading. There are numerous troughs and furrows in this part of the landslide, and only in a few places, as shown in figure 14, can they be shown to be locations of active movement.

Interpretation of displacement rate of the north part of zone 6 is difficult. The displacement progressively diminishes along the major dividing strike-slip fault from 2.8 m/yr near point *N* to 2.5 m/yr just downhill from the first division of the fault. Annual displacement rate decreases to 1.7 m/yr about 50 m further downhill. This change in displacement rate, however, reflects movement of the south side of the major strike-slip fault relative to the north side. Movement rate of material on the north side of the fault near point *P* relative to the boundary is unknown. Farther downhill, where the major fault divides into three parts, more displacement is transferred to the oblique-slip faults on the north side such that two fault-bounded blocks along the line *Q-Q'* and north of the major fault are displaced 1.1 and 1.6 m/yr.

The part of the landslide that is south of the major internal strike-slip fault contains two bands of internal toes that represent shortening of landslide material (fig. 11). One band of toes is the thrust fault described above as part of zone 5, the pond sediments and emergent toe. This band,

about 80 m wide, begins near point *N'* and extends obliquely across the landslide. Within this band, the thrust faults consist of individual, overlapping fault segments. Based on the change in annual displacement (fig. 11), there is more than 1 m/yr of shortening across this internal toe.

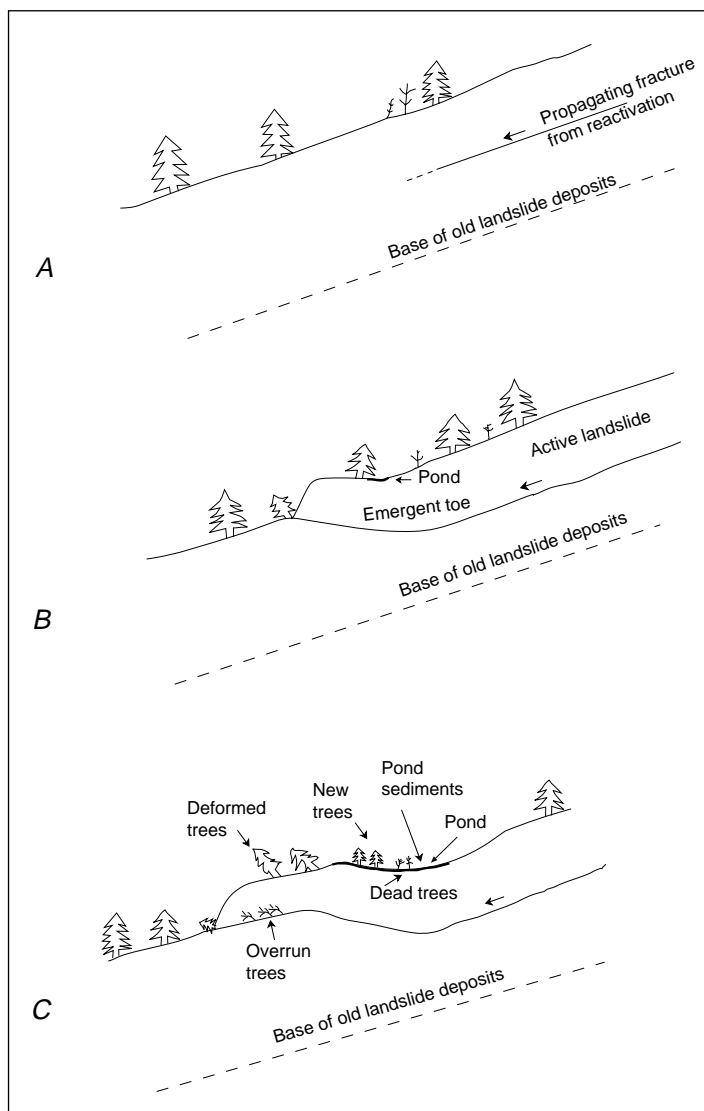**Figure 13.** Sketch of concept of pond formation in conjunction with emergent toe of reactivated movement. *A,* Collapse of rim of Mesa Seco triggers a reactivation of movement. *B,* Failure propagates to region between O to O' and P to P' (fig. 11) where the failure surface emerges to the ground surface. *C,* The features present on the surface of the landslide are a direct result of the geometry of the buried failure surface.

The next band of thrust faults begins along the south flank about 80 m downhill from point *P'*. The thrusting is confined to a much narrower band, and many of the shortening features within the band may be inactive. The band consists of a northwest-trending thrust fault that apparently connects to the south flank and extends continuously into the land-slide body for about 60 m. There it steps along a left-lateral strike-slip fault to another thrust fault that extends to the major internal strike-slip fault zone. The amount of shortening across this band is small. Rate at the downslope toe of the landslide near point *R'* is 1.9 m/yr, and uphill from the inter-nal toe (between *Q* and *Q'*) it is 2.1 m/yr. Thus, annual shortening across this internal toe is appar-ently only about 0.2 m/yr.

Figure 14. View of split tree. The tree is broken into four parts by right-lateral and spreading movement. Fault that caused rupture of tree has not fractured ground surface, but it does form a linear trough about 1 m deep.

Zone 7—Active Toe

The active toe is the downhill terminus of the active landslide beginning near point *O* and contin-uing all the way around the perimeter, *O-P-Q-R'-Q'* (fig. 11, sheet 3). Everywhere along the perimeter, the toe is advancing across the surface of the old, inactive landslide. In the process of overriding the landscape, it pushes trees over and engulfs them into the base of the landslide (fig. 15).

At the toe the thickness of the active landslide is equal to the height of the landslide above the pro-jected surface of the old, inactive landslide. Parise and Guzzi (1992) used this observation to estimate the volume of the active landslide at about 20×10^6 m^3. The volume estimation was based on the thick-ness of the active landslide at the toe combined with displacement vectors and slope to compute the vol-ume of segments of the landslide uphill from the toe. The total volume was obtained by summation (Parise and Guzzi, 1992).

The active toe has an irregular trace along its northern half. Superficial sliding along the over-steepened front of the toe has obscured fractures, so it is not possible to observe causes for the irregulari-ties. We assume that the steps and bends along the terminus are a result of a velocity discontinuity. At many of the irregularities, one of the oblique-slip faults can be projected to the general area of the assumed velocity discontinuity.

The annual displacement rate was measured at seven points around the perimeter of the toe between *Q* and *Q'*. All the measurements except the value of 1.3 m/yr near the terminus were measured by taping distances between wooden stakes. All the measured distances are minimum values because of possible differences between measurement and movement directions. The value of 1.3 m/yr obtained by surveying mentioned above is also a minimum because measurement points extended only about 10 m onto actively moving material.

In the place on the active toe where we were measuring displacement rate by surveying rather than simply taping distances, we were able to deter-mine the displacement vector of the active toe rela-tive to nonmoving ground farther downhill. We expected that the displacement would be approxi-mately parallel to the slope because it is advancing over old landslide debris. To our surprise, we found that the displacement vector is directed nearly hori-zontally out of the slope. This condition, which tends to thicken the toe, may be the result of accu-mulation of trees and other debris along the contact

between moving and nonmoving ground (fig. 15). Displacement tends to steepen the front of the active toe. Sloughing of materials on the oversteepened face gives rise to a churning of material along the active front, and the advance is similar to the motion of the tread of a bulldozer. Continuing movement results in continuing thickening of the toe.

SUMMARY OF KINEMATIC DESCRIPTION OF THE ACTIVE LANDSLIDE

We have divided the active part of the Slumgullion landslide into seven zones, each having a different kinematic expression. Figure 16*A* is a summary sketch of the principal structures on the landslide that have been described. Figure 16*B* shows the same kinematic elements as figure 16*A*, but includes contours of displacement rate. Note that the contours in figure 16*B* are discontinuous across the major structural features on the landslide. It is possible to identify the sense of deformation across a given fracture by the difference in displacement rate on opposite sides of the fracture. For example, the internal strike-slip fault in zone 6 (fig. 11) that separates the slower north side from the faster south side can be readily identified as right lateral on the basis of displacement rate differences alone. Likewise, small landslides superimposed on the larger, active landslide can be identified by closed contours of displacement rate in the hopper, zone 3, and at the

downhill end of zone 4. In general, the displacement-rate contours support the kinematic descriptions in the preceding sections. However, the contours were drawn after we had completed the mapping, and they were not independently drawn. An example of a contour map of displacement rate drawn without information about internal kinematics of the landslide is in Smith (1993).

The uppermost part of the landslide shown by a shaded pattern on fig. 16*A* is the block of landslide material that remains following collapse of part of Mesa Seco. Within the lower part of this remnant block there are a series of scarps that face both uphill and downhill. These scarps represent the head of the currently active landslide (zone 1). Over the next 900 m downslope (zone 2), the landslide is characterized by scarps oriented perpendicular to the direction of movement that indicate stretching. The boundaries of the landslide are curved in this zone, and part of the displacement is carried by internal strike-slip faults that connect the scarps with the flanks. The downslope end of this zone marks the end of simple stretching of the landslide materials. The annual displacement over this reach increases from about 0.5 to 3 m/yr.

The form of the landslide changes dramatically at the hopper. Here the landslide narrows abruptly from 230 to 180 m over a distance of 150 m. Material along the flanks is tilted toward the center of the landslide, and fresh material has been extruded to

Figure 15. View of north side of active toe (zone 7), where trees are being over-ridden by bulldozer-like movement of landslide. Moving ground on left pushes trees over and buries them.

the ground surface adjacent to the bounding strike-slip faults. Within this zone nearly all the trees on the surface of the landslide are destroyed.

Downhill from the hopper and neck and point of maximum displacement the landslide becomes wider over a zone nearly 900 m long (zone 4). The widening is accomplished by the landslide boundary curving outward and producing pull-apart basins. The basins form adjacent to the landslide flanks and are filled by material transported obliquely to the overall direction of sliding. The filling of the basins is the result of differential movements along faults rather than intense internal deformation such as occurs in the hopper. Over the 900-m zone of widening the displacement rate decreases from about 5 m/yr to 3-3.5 m/yr.

The next zone of distinct kinematic features on the surface of the active landslide is an expression of shortening in the lower part of the landslide (zone 6). It is basically the counterpart to zone 2, which contains structures that accommodate stretching. Here most of the shortening occurs within two zones of internal toes. The upper internal toe in the landslide is expressed as a thrust fault and absorbs more than 1 m/yr of shortening. The next internal toe is less active and absorbs less than 0.2 m/yr of shortening. Fractures in these internal toes consist of overlapping segments of thrust faults that make up a zone several tens of meters wide.

At the lower edge of the upper internal toe is an area of extensive pond deposits (zone 5). The pond deposits extend downslope as a trail of pond-laid sediments at least 250 m long as a continuous layer and for as much as 500 m as a broken, discontinuous zone (Van Horn, written commun., 1994). The location of the pond has apparently remained fixed in time, and landslide debris has been transported through the pond, receiving a coating of pond sediments in the process. The surface of the landslide is tilted upslope where the pond has formed. The surface crosses a broad divide and is tilted downslope the rest of the way to the active toe. The pond is speculated to be the position of the toe of the active landslide when it formed in older landslide deposits between 200 and 300 yr ago. The toe apparently emerged here and advanced farther downslope over the older landslide surface (fig. 13). The advance of this part of the landslide has been bulldozer-like, pushing over trees and engulfing them in the base of the active landslide as it moves. Resistance to sliding through the zone containing the buried trees may contribute to an apparent thickening of the landslide at the front of the active toe. Displacement

vectors were not parallel with the slope at the active toe, but rather they were about horizontal. The downhill face of the landslide is covered with nearly continuous superficial slides, adding to the impression that movement at the toe is somewhat analogous to movement of the tread of the bulldozer.

The strike-slip fault that bounds the landslide on the north flank divides into several faults of oblique slip as it approaches the toe. Material north of this fault is advancing over old landslide deposits by sliding and spreading. Spreading is accommodated by numerous oblique-slip faults in the zone. South of this fault material is advancing by sliding downhill over the old landslide deposits. Differential displacement within the landslide here is accommodated by slip along internal strike-slip faults. The shape of the active toe (zone 7) is a crude velocity profile across the distal end of the active landslide. The maximum rate of movement at the toe is about 2 m/yr compared to about 0.8 m/yr on the north and south edges.

SPECULATIONS ABOUT FUTURE MOVEMENT

FACTORS THAT MAY AFFECT FUTURE MOVEMENT

The internal deformation and morphology of the active Slumgullion landslide provide information that can be applied to speculate on future behavior of the landslide. Most of the observations about landslide kinematics indicate that the landslide will stop moving or continue moving at the current rate indefinitely. The kinds of information described above are not ordinarily applied to assess future behavior. However, we believe that part of the value of making observations of kinematic behavior is to assess future behavior, and we offer the following as an experimental methodology.

Displacement Rate

Most observations of rate of movement suggest that the Slumgullion landslide has been moving at an approximately constant rate for at least 30 yr and perhaps more than 100 yr. A wooden stake still remaining on the landslide from the study of Crandell and Varnes (1961) was found near the left flank in zone 4, pull-apart basins (sheet 2). Displacement of that stake, averaged over about 30 yr, was 4.4 m/yr. Measurements of displacement rate in the same area by Smith (1993) result in slightly smaller values in this part of the landslide for the period 1985-90. A measurement by us in 1992-93 along the

27

A

EXPLANATION

Strike-slip shear zone—Arrow indicates relative movement, dashed where uncertain

Scarp—Hachures on downthrown side, dashed where uncertain

Toe—Sawteeth on upper plate

Anticlinal soft-sediment fold

4.0   Average rate of movement, in meters per year

Zone 1, head

Remnant landslide following collapse of north side of scarp

Zone 2, broad bands of scarps and tension cracks

Internal toes

Rotational block movement

Structures that accommodate bending

0.2   0.5   0.8   1.4   1.6   2.5   4.0

Hopper

Zone 3, hopper and neck (structures that accommodate narrowing)

5.8

Neck

4.5

Axial right-lateral shear zone

Zone 4, pull-apart basins (structures that accommodate widening)

3.6

Zone 5, pond deposits and emergent toe

2.5

Zone 6, structures that accommodate spreading

Zone 7, active toe

1.5   2.0

N

0   500 meters

0   1,500 feet

Figure 16 (above and facing page). Summary maps of principal landslide elements shown in two ways. A, Map showing main kinematic features and generalized annual displacement rate of active landslide. Recognition of the elements was based on mapping. B, Contours of annual displacement in meters, drawn based in part on the recognition of main kinematic features of landslide. Displacement-rate gradients identify the expected forms of deformation. Differences in displacement rate across faults provide generalized estimates of movement on the faults. Insufficient data to draw contours in neck, where annual displacement approaches 6 m/yr.

28

B

EXPLANATION

Strike-slip shear zone—Arrow indicates
   relative movement, dashed where
   uncertain

Scarp—Hachures on downthrown side,
   dashed where uncertain

Toe—Sawteeth on upper plate

Anticlinal soft-sediment fold

Isopleth showing average rate of movement—
   Contour interval 0.5 m/yr

Approximate position of maximum measured
rate of displacement, 7.4 m/yr

N

0   500 meters

0   1,500 feet

29

landslide flank, a few meters downhill from the Crandell and Varnes stake, gave a larger value of nearly 4.9 m/yr. For our purposes, these differences are insignificant because they were measured at different places in different ways. The old photographs taken of the active landslide by Cross (Howe, 1909) show the landslide looking much the same more than 80 yr ago as it does today. On the basis of these observations, one could conclude that the annual movement has been and will continue to be about steady.

More precise measurements over a shorter term, however, indicate that the displacement rate is variable. Gomberg and others (1995) measured displacement rate with ultra-sensitive creep meters while attempting to detect and locate sources of bursts of micro-seismic energy release from within the actively moving landslide. Small triggered-creep events were set off by small explosions several tens of meters away; the explosions were being used to calibrate the velocity structure for location of sources. The creep record (Gomberg and others, 1995) indicated that the triggered slip is an excursion from a steady rate. The small explosions caused an abrupt increase in slip followed by a few minutes of slower-than-average slip with the net result a steady rate of creep in a record about 30 min long. The magnitude of the triggered slip events was a few tenths of millimeters, and the entire slip recovery lasted about 5 min for each of two tests. These results do not provide information to predict long-term behavior other than to support steady-state movement.

Measurements by Savage and Fleming (1996) were made using recording extensometers on the south flank of the landslide near the point of most rapid movement in the neck. Here the maximum rate was 11.6 m/yr in early May 1993. The minimum, measured in early April 1993 when the ground was frozen, was 2.75 m/yr. The average rate from April 1993 to March 1994 was 5.84 m/yr.

The observation that the displacement rate varies shows that movement rate is sensitive to seasonal changes within the landslide. Baum and others (1993) noted the same phenomenon at the Aspen Grove landslide in Utah and were able to correlate the slowing and cessation of movement with a decrease in water levels in borings. These seasonal changes apparently are due to freezing of the ground surface that reduces infiltration and causes a concurrent change in subsurface water pressures.

Based on previous work (Crandell and Varnes, 1961) and before the precise measurement of dis-placement rate at Slumgullion by Savage and Fleming (1996), we believed that the movement rate was steady at each point on the surface of the landslide. At that time, we speculated that an increase in subsurface water level would be buffered by an increase in surface-water discharge and vice versa. We observed through the study period that the level of water in surface ponds on the landslide has remained about constant as has the discharge of surface water from the toe of the landslide. While this may be true for part of the year, the prolonged winter freeze contributes to a dramatic decrease in rate of movement just before the ground thaws in the spring.

The point of describing these observations is that we now recognize that the landslide rate is sensitive to seasonal change, and movement could reasonably be expected to change in the event of prolonged drought or high precipitation. If the feedback mechanism described above is significant, an increase in precipitation might be less effective in accelerating movement than a drought in slowing movement. Acceleration would be buffered by increased surface runoff from the landslide. Slowing could occur if the amount of surface water on the landslide diminished to the point that the subsurface water could not be replenished.

While the displacement data are interesting, they have very little value in predicting the future behavior of the landslide. Probably the most significant observation is that the displacement rate does change seasonally and, thus, is subject to change annually, given a change in one or more of the factors that control the rate of movement.

Change in Resistance to Sliding at the Toe

Four features associated with the active landslide toe indicate that resistance to sliding is increasing. First, the displacement vector along the front of the active toe is horizontal rather than parallel to the slope. Horizontal displacement implies thickening of the toe and added resistance to sliding. Second, the toe is divisible into two kinematic elements separated by the major internal strike-slip fault described in the section on spreading. The part of the toe that is north of the strike-slip fault is spreading laterally as well as advancing downslope; displacement is along oblique-slip faults. Spreading also adds resistance. Third, downhill from the active toe the active landslide must override the surface of older landslide deposits from an earlier landslide episode. The slope of this surface contains local benches and ramps but

overall is becoming flatter. For the next 100 m or more downhill from the active toe there is a local bench that produces a flatter slope than average. And, fourth, the shape in plan view of the toe to the south of the major internal strike-slip fault is becoming more point shaped because of differences in displacement rate around the perimeter. At some time this part of the toe will become so thick and so narrow that it will also begin to spread laterally.

Change in Supply of Materials

Beginning in the upper part of the landslide near *E-E'* (fig. 5) and extending 2 km downhill, the surface of the active landslide is topographically lower than the inactive deposits that bound the active part of the landslide. This topographic trough that contains the active landslide extends downslope on the left flank to a point about 50 m uphill from point *L'* and on the right flank to a point about 100 m uphill from point *M* (fig. 8). The surface of the active landslide uphill from these points is typically about 3 m lower than the top of the inactive flank ridges that are adjacent to the moving ground. Downhill from these points, the active landslide is topographically elevated with respect to nonmoving ground adjacent to its flanks. The amount of positive elevation change is particularly large on the south flank between points *O'* and *Q'* (fig. 11) where the landslide is constrained by the valley of Slumgullion Creek. The height of landslide deposits with respect to the valley floor is about 12 m. The continued increase of resisting forces on the downhill side of the line between points *M* and *L'* (fig. 8) should, over the long term, halt the movement. Duncan and others (1986) noted a similar depletion of materials in the upper part and accumulation of materials in the lower part of the Thistle landslide in Utah. There the upper part of the landslide was bounded by a scarp nearly 30 m high.

Local changes in the surface of the landslide were studied with sequential aerial photography. The pull-apart basin on the north flank between points *J* and *K* (fig. 8), was examined to further study the apparent redistribution of material from the upper to the lower part of the landslide. Loss of material in the upper part represents a decrease in driving force, and gain of material in the lower part represents an increase in resisting force. If the pull-apart basin is becoming deeper or larger, the apparent loss of driving force is continuing. Topographic maps having a 2-m contour interval were prepared of the landslide from 1985 and 1990 sets of photographs. Contour

data were stored digitally. Philip Powers compared the digital data for the topography in the pull-apart basin. The method involved computing the void space from the ground surface in the basin to a planar surface fitted to the upper, topographic perimeter of the basin. The 1985 and 1990 data were compared to the same upper planar surface and the volume computed from a 2-m-spaced grid of points over the entire basin. The volume of the void above the basin was 39,300 m^3 in 1985 and 41,300 m^3 in 1990; net change was 2000 m^3 of basin enlargement. The loss of material from the basin is consistent with our other observations that driving forces are diminishing.

FUTURE MOVEMENT OF THE SLUMGULLION LANDSLIDE

The changes in morphology of the landslide and the movement record for the toe are evidence that the landslide is in the process of stopping rather than accelerating. All the kinematic data that we believe relevant to predict the future movement imply both reduced driving forces and increased resisting forces.

Even though some evidence supports a steady state for long-term movement, extensometer measurements show that the rate varies seasonally. Thus, future movement rates will be strongly dependent on subsurface water pressures. Very wet or dry periods might change the rates significantly over the short term, but the changes in morphology that are leading to an end of movement should dominate in the longer term. The time frame for an end to this episode of active movement is even less certain than our conclusion that the movement will stop. Over the near term, perhaps decades, we expect movement to continue.

Another collapse of the rim of Mesa Seco could rejuvenate the sliding. At present there is no evidence for an impending collapse such as the one that triggered the current activity. Thus, we conclude that the current episode of movement will run its course without catastrophic effects on Lake Fork.

This study, while a broad overview of displacement and kinematics of the active Slumgullion landslide, left many interesting topics unexplored. In this section, a few of these unexplained topics are listed with the hope that they might be of interest to future researchers.

The landslide should be rephotographed and remapped. This map provides a base line of displacement, kinematic, and structural information that might change in interesting ways in the future.

This map was based on aerial photographs and topography as of 1990. Many of our inferences about fixed positions of structures on the landslide surface and changes in driving and resisting forces could readily be tested.

We recognized but have not described areas where materials from the subsurface have been extruded onto the ground surface. The mechanics of such extrusion may be discernable from the kinematic setting of the extrusions. We observed active extrusions in the hopper, where landslide materials are moving into the most narrow part of the landslide. The extrusions there are along the landslide flanks. The deposits of extrusion were evident in other places where their kinematic setting was not clear.

Likewise, we found tabular dikes of highly plastic clay (liquid limit=110, plasticity index=75) intruded into the landslide debris at several locations in the landslide. Similar intruded dikes were reported in the Twin Lake landslide in Utah by Fleming and Johnson (1989). This clay is apparently the weakest material in the landslide, and intrusions of clay dikes along fault zones could facilitate movement.

Individual structures such as pull-apart basins, flank ridges, shear zones, and different types of faults are amenable to detailed study that would reveal how they form. The formation could be derived from precise surveys and measurements of deformation using quadrilaterals (Baum and others, 1988). Qualitative information on kinematic history of the landslide could be obtained from a study of tilted trees and stretched roots.

And, finally, there have been no systematic observations about surface and subsurface water on the Slumgullion landslide.

A major advantage to research at the Slumgullion landslide is its history of continuing movement—day to day, decade to decade. Measurements can be made to test models of fracturing and distortion in different situations that have a good chance of providing a long record of data. While we believe that the landslide will stop moving in the long term, it is not yet clear when that might be.

Acknowledgments—We especially acknowledge the contributions of Rafaella Guzzi, who tragically lost her life in an automobile accident in Italy in 1994. Rafaella participated in many of the preliminary studies of the Slumgullion landslide including establishment of the survey control and mapping of structures in the active landslide. Her dedication to geology, good humor, and charm were a special reward for everyone who worked with her.

We also appreciate the assistance and efforts of the other exchange students sponsored by the Italian Research Council, including Mario Parise, Giovani Crosta, Marta Chiarle, and Guzzi's and Parise's academic sponsor, Professor Marino Sorriso-Valvo. We also appreciate the assistance of the USGS Plotter Lab staff and James Messerich in the preparation of the base map and development of the means to measure displacement from sequential aerial photographs. Other USGS colleagues that supplied data and information useful to this mapping effort were David and Katherine Varnes, William Savage, William Smith, and Robert Schuster. Philip Powers computed the volume change in a pull-apart basin. Jack Odum helped establish the displacement-monitoring arrays. William Smith provided data on displacement in digital form. Duane Eversol of the Nebraska Geological Survey helped us in the field and with surveying. Arvid Johnson of Purdue University and Jeff Coe provided thorough and critical reviews of the map and text. And, finally, Richard Walker of Lake City provided hospitality and help wherever and whenever it was needed. To all these people, we express our sincere thanks.

REFERENCES CITED

Atwood, W.W., and Mather, K.F., 1932, Physiography and Quaternary geology of the San Juan Mountains, Colorado: U.S. Geological Survey Professional Paper 166, 176 p.

Baum, R.L., and Fleming, R.W., 1991, Use of longitudinal strain in identifying driving and resisting elements of landslides: Geological Society of America Bulletin, v. 103, p. 1121-1132.

Baum, R.L., Fleming, R.W., and Ellen, S.D., 1989, Maps showing landslide features and related ground deformation in the Woodlawn area of the Manoa Valley, City and County of Honolulu, Hawaii: U.S. Geological Survey Open-File Report 89-290, 16 p., 2 pls.

Baum, R.L., Fleming, R.W., and Johnson, A.M., 1993, Kinematics of the Aspen Grove landslide, Ephraim Canyon, central Utah, chap. F *of* Landslide processes in Utah—Observation and theory: U.S. Geological Survey Bulletin 1842, p. F1-F34.

Baum, R.L., Johnson, A.M., and Fleming, R.W., 1988, Measurement of slope deformation using quadrilaterals, chap. B *of* Landslide processes in Utah—Observation and theory: U.S. Geological Survey Bulletin 1842, p. B1-B23.

Burbank, W.S., 1947, Lake City area, Hinsdale County, *in* Mineral resources of Colorado: Colorado Mineral Resources Board, p. 439-443.

Chleborad, A.F., 1993, Description, origin, and implications of a newly identified Slumgullion landslide deposit, San Juan Mountains, southwestern Colorado: U.S. Geological Survey Open-File Report 93-548, 16 p.

Crandell, D.R., and Varnes, D.J., 1960, Slumgullion earthflow and earthslide near Lake City, Colorado [abs.]: Geological Society of America Bulletin, v. 71, no. 12, pt. 2, p. 1846.

———1961, Movement of the Slumgullion earthflow near Lake City, Colorado, art. 57 *in* Short papers in the geologic and hydrologic sciences: U.S. Geological Survey Professional Paper 424-B, p. B136-B139.

Diehl, S.F., and Schuster, R.L., 1996, Preliminary geologic map and alteration mineralogy of the main scarp of the Slumgullion landslide, chap. 3 *in* Varnes, D.J., and Savage, W.Z., eds., The Slumgullion earth flow—A large scale natural laboratory: U.S. Geological Survey Bulletin 2130, p. 13-19.

Duncan, J.M., Fleming, R.W., and Patton, F.D., 1986, Report of the Thistle Slide Committee to the State of Utah, Department of Natural Resources, Division of Water Rights: U.S. Geological Survey Open-File Report 86-505, 95 p., 8 pls.

Endlich, F.M., 1876, Report of F.M. Endlich, *in* U.S. Geological and Geographical Survey (Hayden) of the Territories Annual Report 1874, p. 203.

Fleming, R.W., Baum, R.L., and Johnson, A.M., 1993, Deformation of landslide surfaces as indicators of movement processes, *in* Proceedings of the 2nd Seminar on Landslide Hazards, Cosenza, Italy, March 5-6, 1990: Geographica Fisica e Dinamica Quaternaria, v. 16, no. 1, p. 9-11.

Fleming, R.W., Baum, R.L., and Savage, W.Z., 1996, The Slumgullion landslide, Hinsdale County, Colorado, *in* Colorado Geological Survey Special Publication 44: Geological Society of America Guidebook for Field Trips, 108th Annual Meeting, Denver, Colo., 1996, 23 p. (Available on CD-ROM from the Colorado Geological Survey, 1313 Sherman Street, Denver, CO.)

Fleming, R.W., and Johnson, A.M., 1989, Structures associated with strike-slip faults that bound landslide elements: Engineering Geology, v. 27, p. 39-114.

Fleming, R.W., Johnson, R.B., and Schuster, R.L., 1988, The reactivation of the Manti landslide, chap. A *of* The Manti, Utah landslide: U.S. Geological Survey Professional Paper 1311, p. 1–22, 1 pl.

Gilbert, G.K., 1928, Studies of basin-range structure: U.S. Geological Survey Bulletin 324, p. 1-13.

Gomberg, J.S., Bodin, P.W., Savage, W.Z., and Jackson, M.E., 1995, Landslide faults and tectonic faults, analogs? The Slumgullion earthflow, Colorado: Geology, v. 23, no. 1, p. 41-44.

Guzzi, Rafaella, and Parise, Mario, 1992, Surface features and kinematics of the Slumgullion landslide near Lake City, Colorado: U.S. Geological Survey Open-File Report 92-252, 45 p.

Howe, Ernest, 1909, Landslides in the San Juan Mountains, Colorado: U.S. Geological Survey Professional Paper 67, 45 p.

Johnson, A.M., and Fleming, R.W., 1993, Formation of left-lateral fractures within the Summit Ridge shear zone, 1989 Loma Prieta, California, earthquake: Journal of Geophysical Research, v. 98, no. B12, p. 21823-21837.

Johnson, A.M., Fleming, R.W., and Cruikshank, K.M., 1994, Shear zones formed along long, straight traces of fault zones during the 28 June 1992 Landers, California, earthquake: Bulletin of the Seismological Society of America, v. 84, p. 499-510.

Johnson, A.M., Fleming, R.W., Cruikshank, K.M., Martosudarmo, S.Y., Johnson, N.A., Johnson, K.M., and Wei, Wei, 1997, Analecta of structures formed during the 28 June 1992 Landers-Big Bear, California earthquake sequence: U.S. Geological Survey Open-File Report 97-94, 7 pls., 59 p.

Larsen, E.E., 1913, Alunite in the San Cristobal quadrangle, Colorado: U.S. Geological Survey Bulletin 530-F, p. 179-183.

Lipman, P.W., 1976, Geologic map of the Lake City caldera area, western San Juan Mountains, southwestern Colorado: U.S. Geological Survey Miscellaneous Investigations Series Map I-962, scale 1:48,000.

Madole, R.F., 1996, Preliminary chronology of the Slumgullion landslide, Hinsdale County, Colorado, chap. 1 *in* Varnes, D.J., and Savage, W.Z., eds., The Slumgullion earth flow—A large scale natural laboratory: U.S. Geological Survey Bulletin 2130, p. 5-8.

Parise, Mario, and Guzzi, Rafaella, 1992, Volume and shape of the active and inactive parts of the Slumgullion landslide, Hinsdale County, Colorado: U.S. Geological Survey Open-File Report 92-216, 29 p.

Savage, W.Z., and Fleming, R.W., 1996, Slumgullion landslide fault creep studies, chap. 12 *in* Varnes, D.J., and Savage, W.Z., eds., The Slumgullion earth flow—A large scale natural laboratory: U.S. Geological Survey Bulletin 2130, p. 83-87.

Smith, W.K., 1993, Photogrammetric determination of movement on the Slumgullion slide, Hinsdale County, Colorado, 1985-1990: U.S. Geological Survey Open-File Report 93-597, 17 p., 2 pl.

Varnes, D.J., and Savage, W.Z., eds., 1996, The Slumgullion earth flow—A large scale natural laboratory: U.S. Geological Survey Bulletin 2130, 95 p.